Ore Geology Reviews 90 (2017) 131–147

Contents lists available at ScienceDirect

Ore Geology Reviews

journal homepage: www.elsevier.com/locate/oregeo

Thick chromitite of the Jacurici Complex (NE Craton São Francisco, Brazil): Cumulate chromite slurry in a conduit

Juliana Charão Marques [a,*], João RodrigoVargas Pilla Dias [a], Betina Maria Friedrich [a], José Carlos Frantz [a], Waldemir José Alves Queiroz [b], Nilson Francisquini Botelho [c]

[a] Instituto de Geociências, Universidade Federal do Rio Grande do Sul, Av. Bento Gonçalves 9500, Prédio 43129, Porto Alegre, RS CEP 91501-970, Brazil
[b] Companhia de Ferro Ligas da Bahia – FERBASA, Pojuca, BA, Brazil
[c] Instituto de Geociências – Universidade de Brasília, Brazil

ARTICLE INFO

Article history:
Received 31 July 2016
Received in revised form 26 April 2017
Accepted 30 April 2017
Available online 3 May 2017

Keywords:
Chromite deposit
Mafic-ultramafic layered complex
Chromite slurry
Conduit

ABSTRACT

The Jacurici Complex, located in the NE part of the São Francisco Craton, hosts the largest chromite deposit in Brazil. The mineralized intrusion is considered to be a single N-S elongated layered body, disrupted into many segments by subsequent deformation. The ore is hosted in a thick, massive layer. Two segments, Ipueira and Medrado, have been previously studied. We provide new geological information, and chromite composition results from the Monte Alegre Sul and Várzea do Macaco segments located farther north, and integrate these with previous results. The aim of this study is to determine and discuss the magma chamber process that could explain the formation of the thick chromitite layer. All segments exhibit similar stratigraphic successions with an ultramafic zone (250 m thick) hosting a 5–8 m thick main chromitite layer (MCL), and a mafic zone (40 m thick). The chromite composition of the MCL, *Mg*-numbers (0.48–0.72) and *Cr*-numbers (0.59–0.68), is similar to chromites from layered intrusions and other thick chromitites. Previous work concluded that the parental magma of the mineralized intrusion was very primitive based on olivine composition (up to Fo_{93}) and orthopyroxene composition (up to En_{94}) from harzburgite samples, and that it originated from an old subcontinental lithospheric mantle. We estimate that the melt from which the massive chromitite layer crystallized was similar to a boninite, or low siliceous high-Mg basalt, with a higher Fe/Mg ratio. The petrologic evidence from the mafic-ultramafic rocks suggests that a high volume of magma flowed through the sill, which acted as a dynamic conduit. Crustal contamination has previously been considered as the trigger for the chromite crystallization, based on isotope studies, as the more radiogenic signatures correlate with an increase in the volumetric percentage of amphibole (up to 20%). The abundant inclusions of hydrous silicate phases in the chromites from the massive ore suggest that the magma was hydrated during chromite crystallization. Fluids may have played an important role in the chromite formation and/or accumulation. However, the trigger for chromite crystallization remains debatable. The anomalous thickness of the chromitite is a difficult feature to explain. We suggest a combined model where chromite crystallized along the margins of the magma conduit, producing a semi-consolidated chromite slurry that slumped through the conduit forming a thick chromitite layer in the magma chamber where layered ultramafic rocks were previously formed. Subsequently, the conduit was obstructed and the resident magma fractionated to produce a more evolved composition.

1. Introduction

Chromite has long been used as a petrogenetic indicator (Irvine, 1967; Barnes and Roeder, 2001; Stowe, 1994), even when affected by strong regional deformation (Barnes and Jones, 2013). It is especially reliable when hosted in massive chromitites, due to the low degree of sub-solidus exchanges in monomineralic layers (Sack and Ghiorso, 1991). The formation of massive chromitite has been the subject of many studies, and the origin remains debatable. Different models have already been considered and discussed (see reviews by Maier et al., 2013; Mondal and Mathez, 2007; Naldrett et al., 2012). Nevertheless, there is no consensus as to whether the crystallization occurred in-situ in response to a change in the stability field causing saturation in chromite, or if the chromite was transported and accumulated. We address this

* Corresponding author.
E-mail address: juliana.marques@ufrgs.br (J.C. Marques).

http://dx.doi.org/10.1016/j.oregeorev.2017.04.033
0169-1368/

problem by studying the thick massive chromitite layer from the Jacurici Complex.

The Jacurici Complex hosts the largest chromite deposit in Brazil (Marinho et al., 1986), cropping out along a N-S trending area that is at least 70 km long and 20 km wide in the NE part of the São Francisco Craton (Fig. 1). The ore is mined from a massive chromitite layer, up to 8 m in thickness, hosted in a 300 m thick mafic-ultramafic layered body. The chromitites from the Jacurici Complex have only been previously studied in the Ipueira and Medrado areas (Deus and Viana, 1982; Lord et al., 2004; Marques and Ferreira Filho, 2003; Marques et al., 2003; Mello et al., 1986), where a major mining operation is located. However, there are fifteen mineralized segments along the belt.

The formation of such thick chromitite layers is problematic when mass balance is considered. In order to produce the volume of chromite found in the thick layers, much of the magma responsible for the chromite crystallization must have escaped. Marques and Ferreira Filho (2003) suggested that the magma chamber acted as a conduit in order to explain the enormous amount of chromite hosted in just few meters of silicate cumulate rocks. Here we investigate two segments located farther north, the Monte Alegre Sul and Várzea do Macaco (Fig. 2), to provide new geological information and new chromite compositional analyses. The main aim of this study is to integrate previous information with the new data, in order to discuss magma chamber processes that could explain the formation of the thick chromitite.

2. Tectonic setting

According to Almeida (1977), the São Francisco Craton was produced by the amalgamation of Archean cratons during the Paleoproterozoic Transamazonian Cycle, developing mobile belts and causing severe reworking of the craton margins (Almeida et al., 2000; Barbosa and Sabaté, 2002, 2003; Teixeira et al., 2000). In

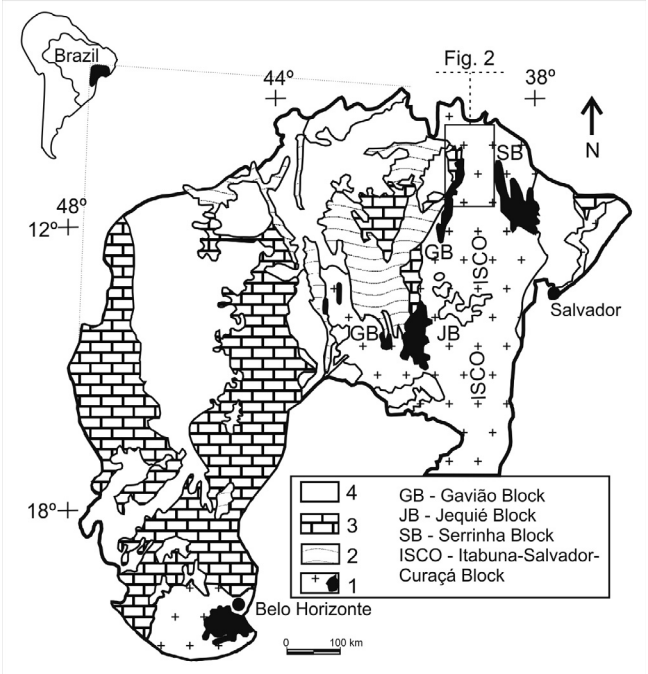

Fig. 1. Generalized map of the São Francisco Craton. (1) Archean/Paleoproterozoic basement with greenstone belt sequences and the Jacobina Group (in black). (2) Mesoproterozoic cover of the Espinhaço Supergroup. (3) Neoproterozoic cover of the São Francisco Supergroup. (4) Phanerozoic cover. Approximate location of Fig. 2 is shown. Adapted from Barbosa et al. (2003).

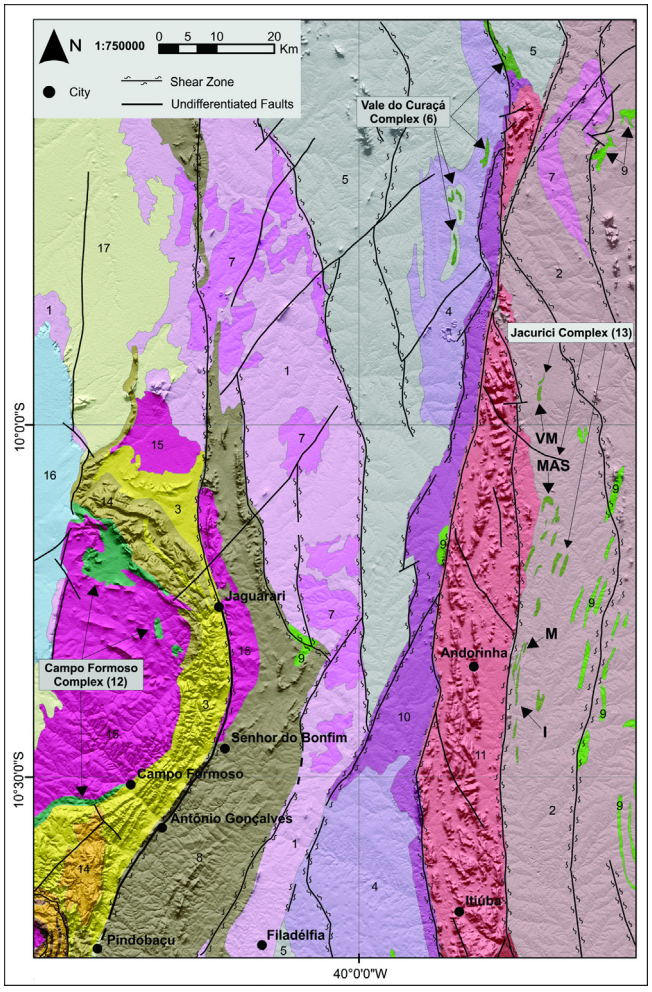

Fig. 2. Geologic setting of the Jacurici Complex (simplified from Kosin et al., 2004). The location of the Ipueira (I), Medrado (M), Monte Alegre Sul (MAS) and Várzea do Macaco (VM) segments are indicated. Lithostratigraphic units: Paleoarchean – (1) Basement rocks; Mesoarchean – (2) Santa Luz Complex; Neoarchean – (3) Itapicuru Complex; (4) Caraiba Complex; (5) Tanque Novo-Ipirá Complex; (6) Vale do Curaçá Complex; (7) Undifferentiated granitoids; Paleoproterozoic – (8) Saúde Complex; (9) Undifferentiated mafic-ultramafic bodies; (10) Riacho da Onça Granitoid: (11) Itiúba Syenite; (12) Campo Formoso Complex; (13) Jacurici Complex; (14) Jacobina Group; (15) Campo Formoso and Jaguari's region granitoids; Neoproterozoic – (16) Salitre Formation; Cenozoic – (17) Sedimentary cover.

the northern segment where the Jacurici Complex is located (Fig. 2), the amalgamation of two major Archean blocks, the 3.4 to 3.1 Ga Gavião (Barbosa and Dominguez, 1996; Martin et al., 1997; Santos-Pinto et al., 1998) and the 3.1 to 2,7 Ga Serrinha (Barbosa et al., 2012; Brito Neves et al., 1980; Cordani et al., 1999; Oliveira et al., 1999, 2002; Silveira et al., 2015) produced the highly deformed and metamorphosed Salvador-Curaçá mobile belt (Santos and Souza, 1983), or the Itabuna-Salvador-Curaçá orogen when considering its extension to the south (Barbosa and Dominguez, 1996; Oliveira et al., 2004). The age of the metamorphic peak is not well constrained and is estimated to be around 2.3–2.1 Ga (Barbosa et al., 2012; Kosin et al., 2003), but the end of shearing is marked by the age of alkaline granitoid intrusions, which vary from 2.08 to 2.07 Ga (Oliveira et al., 2004; Silveira et al., 2015). Barbosa et al. (2012) and Kosin et al. (2003) reviewed the tectonic evolution of the craton and its lithologies, and a brief summary is given below.

The Serrinha Block is considered to be a granite-greenstone belt formed by the Archean Uauá and Santa Luz Complexes. The Uauá Complex is located at the extreme northeast end of the block and

is composed of tonalitic to granodioritic gneiss. It is considered to be the oldest part of the block, with ages varying from 2.93 to 3.13 Ga based upon U-Pb in zircons (Cordani et al., 1999; Oliveira et al., 1999). The Santa Luz Complex is the largest unit and is constituted by several different types of rocks varying from igneous to sedimentary in origin, mostly metamorphosed under amphibolite facies conditions. The age is considered to vary from 3.0 to 2.7 Ga (Barbosa et al., 2012; Oliveira et al., 2002, 2007; Silveira et al., 2015) with peak metamorphism at 2.1–1.9 Ga (Barbosa et al., 2012; Bastos Leal et al., 1994).

The Salvador-Curaçá Belt comprises the Tanque Novo-Ipirá and the Caraíba complexes. The Tanque Novo-Ipirá Complex is a volcano-sedimentary sequence deformed and metamorphosed under amphibolite to granulite conditions. The Caraíba Complex is composed of granulitic tonalitic to granodioritic gneisses (Oliveira et al., 2004). The available ages point to 2.6 Ga for the Caraíba Complex (Sabaté et al., 1994; Silva et al., 1997, 2002) with peak metamorphism considered to be 2.07–2.08 Ga (Silva et al., 1997).

The Jacurici Complex is part of the heavily denuded remnants of a large igneous province, deformed and metamorphosed during the Paleoproterozoic, which has been described as a swarm of chromite-rich mafic-ultramafic layered sills (Deus and Viana, 1982). The Complex is considered to occur along a trend approximately 70 km long and 20 km wide (Fig. 2), outcropping to the east of and parallel to the Itiúba Syenite, a huge alkaline massif with 150 km of extension emplaced during the late stages of the Paleoproterozoic deformation (Barbosa and Sabaté, 2002; Conceição et al., 1991). Nevertheless, detailed mapping and extensive drilling carried out by the Geology Division of the FERBASA Company demonstrates that the Jacurici Complex is much larger and voluminous than previously considered. Fifteen mineralized mafic-ultramafic segments hosting thick chromitite layers have been explored by FERBASA since 1973. An underground operation at the Ipueira segment is producing circa 360,000 t/year of chromite at 35–40 wt% Cr_2O_3 on average (FERBASA geology division, 2015, internal report). All bodies are composed of similar types of rocks across the stratigraphy. The mafic-ultramafic rocks have been studied in the Ipueira and Medrado segments (Deus and Viana, 1982; Lord et al., 2004; Marques and Ferreira Filho, 2003; Marques et al., 2003), located in the southern part of the belt, and were subsequently reviewed by Ferreira Filho and Araujo (2009).

Oliveira et al. (2004) obtained one SHRIMP U-Pb zircon age of 2085 ± 5 Ma from a mafic rock in the Jacurici intrusions. This age was considered to be the crystallization time, although the zircons showed no typical igneous zonations. This interpretation was based exclusively on the Th/U ratios, which alone do not support such an interpretation considering that Th/U ratios can be variable under high-T metamorphism (Harley and Kelly, 2007; Moller et al., 2003) and depend on multiple factors. The Itiúba Syenite is also considered as having crystallized at 2084 ± 16 Ma (Oliveira et al., 2004), an age regarded as coeval with the last stage of shearing (Kosin et al., 2003). Recently, Silveira et al. (2015) dated a mylonitic alkali granite that crops out near the Jacurici Complex and is coeval to the Itiúba Syenite, obtaining an age of 2081 ± 3 Ma implied to represent the last deformation event in the area. The age of 2.08 Ga for the Jacurici Complex is therefore difficult to reconcile with the metamorphic evolution of the complex, given that it is locally strongly deformed and partially recrystallized, with the metamorphic peak considered to be in amphibolite to granulite facies.

3. Sampling and analytical procedures

Several drill cores were described from three geological sections from the Monte Alegre Sul segment and from six geological sections from the Várzea do Macaco. One representative drill core from each area was selected for sampling. Twenty polished thin sections from the massive chromitites were extensively described and those with preserved minerals and textures were selected for chemical analyses.

Semi-quantitative analyses of major elements were performed using a JEOL 6610-LV scanning electron microscope (SEM), equipped with a Bruker Nano XFlash 5030 energy dispersive spectrometer (EDS) detector at the Laboratório de Geologia Isotópica at the Universidade Federal do Rio Grande do Sul. The aim was to help in the identification of mineral inclusions in chrome-spinels following their recognition in petrographic examinations. The SEM was operated with 15 kV acceleration potential and a 16 mm working distance. The standard ZAF calibration method was applied.

A comprehensive investigation of the chromite compositions of the Ipueira (subdivided in Ipueira Sul and Ipueira II segments) and Medrado segments was performed by Marques (2001) and Marques and Ferreira Filho (2003). New analyses of the Monte Alegre Sul and Várzea do Macaco segments were obtained using a JEOL JXA-8230 electron microprobe at the Universidade de Brasília, following similar analytical procedures to avoid major bias. The equipment was operated with 15 kV acceleration potential and a 20 nA beam current, using natural mineral standards and standard ZAF matrix corrections. Background counting time was set to 5 s. Ferric iron was calculated on the basis of stoichiometry profiles in single grains, which revealed a very homogeneous composition with no zonation and only minor variation near fractures or very close to the external margins, where chromite is in contact with silicates. The analyses used for the trends and diagrams were performed on the homogeneous cores, avoiding any possible disturbance. The results are available in Appendices 1 and 2 and representative data are shown in Table 1. Analyses from the Ipueira (Sul and II) and Medrado segments used in the diagrams are from Marques (2001). Representative data from those areas are available in Marques and Ferreira Filho (2003).

4. Geology and petrography of the Jacurici mineralized complex

The Jacurici mafic-ultramafic rocks show a similar stratigraphic succession in all studied segments and can be subdivided using the same scheme adopted for the Ipueira and Medrado areas (cf. Marques and Ferreira Filho, 2003; Fig. 3), except for the absence of the Marginal Zone at the Monte Alegre Sul and Várzea do Macaco segments which are located farther north, respectively 20–25 km and 35–40 km from the Ipueira underground mine (Fig. 2). The zonal subdivision was mainly based on rock composition, and the thick chromitite layer is hosted in the Ultramafic Zone. The Ultramafic Zone is subdivided into three members: (1) the Lower Ultramafic Unit (LUU); (2) the Main Chromitite Layer (MCL); and (3) the Upper Ultramafic Unit (UUU) (Fig. 3).

A recent drilling campaign intersected a flank in the Ipueira mining area, confirming a tight synformal structure (Fig. 4) which was previously observed in the Medrado area where the fold hinge outcrops. The mafic-ultramafic layers show several sets of later normal faults, offsetting the prominent chromitite (Fig. 4). The stratiform intrusion is conformable with underlying quartz-feldspathic orthogneiss and with overlying metasedimentary rocks that include calc-silicate rocks and marbles. At Monte Alegre Sul (Fig. 5), the layered complex is in an upright position and the overlying rocks comprise a quartz-feldspathic gneiss. No underlying rocks were identified, as drilling was halted just after the chromitites were intersected. At Várzea do Macaco (Fig. 6), the stratigraphy is inverted and generally the overlying rocks are quartz-feldspathic gneiss and the underlying rocks are metasedimentary.

Table 1
Representative chemical compositions of chromite from the Monte Alegre Sul segment (MAS) massive chromitite along the MAS-105-65 borehole and from the Várzea do Macaco segment (VM) massive chromitite along the VM1-88-70 borehole.

Segment	Monte Alegre Sul segment					Várzea do Macaco segment			
Drill core	105-65°	105-65°	105-65°	105-65°	105-65°	88-70°	88-70°	88-70°	88-70°
Unit	MCL	MCL	MCL	MCL	MCL	MCL	MCL	MCL	MCL
Texture	Massive	Massive	Massive	Massive	Massive	Massive	Massive	Massive	Massive
Depth	76.8	78.2	79.1	81.64	82.8	96.78	97.75	98.6	99.64
Oxides in wt. percent									
SiO_2	0.00	0.00	0.00	0.03	0.00	0.00	0.00	0.00	0.00
TiO_2	0.30	0.24	0.25	0.28	0.31	0.24	0.43	0.41	0.35
Al_2O_3	18.80	18.84	16.15	18.23	18.76	20.56	19.49	19.16	19.27
Cr_2O_3	46.96	49.38	50.45	47.76	48.73	47.97	49.63	48.59	48.64
V_2O_5	0.09	0.13	0.08	0.05	0.14	0.12	0.08	0.16	0.09
Fe_2O_3	4.83	3.36	3.83	4.50	3.53	1.93	1.44	2.25	1.78
FeO	15.64	14.06	16.84	15.99	14.51	16.47	16.29	16.64	17.95
MnO	0.26	0.30	0.42	0.32	0.31	0.60	0.59	0.57	0.46
MgO	12.84	13.68	11.83	12.65	13.43	12.25	12.31	12.05	11.35
CaO	0.00	0.00	0.00	0.00	0.00	0.02	0.01	0.02	0.01
ZnO	0.01	0.00	0.00	0.01	0.09	0.00	0.00	0.00	0.00
NiO	0.22	0.13	0.19	0.17	0.21	0.11	0.07	0.09	0.15
Total	99.93	99.97	99.98	100.03	99.98	100.27	100.34	99.95	100.07
Number of cations per 32 oxygens									
Si	0.00	0.00	0.00	0.01	0.00	0.00	0.00	0.00	0.00
Ti	0.06	0.05	0.05	0.05	0.06	0.04	0.08	0.08	0.07
Al	5.56	5.53	4.86	5.41	5.50	6.01	5.71	5.67	5.71
Cr	9.32	9.72	10.18	9.50	9.58	9.41	9.75	9.66	9.67
V	0.02	0.03	0.02	0.01	0.03	0.02	0.02	0.03	0.02
Fe^{3+}	0.91	0.63	0.73	0.85	0.66	0.36	0.27	0.43	0.34
Fe^{+2}	3.28	2.93	3.59	3.36	3.02	3.42	3.39	3.50	3.77
Mn	0.06	0.06	0.09	0.07	0.07	0.13	0.12	0.12	0.10
Mg	4.80	5.08	4.50	4.74	4.98	4.54	4.56	4.51	4.25
Ca	0.00	0.00	0.00	0.00	0.00	0.01	0.00	0.01	0.00
Zn	0.00	0.00	0.00	0.00	0.02	0.00	0.00	0.00	0.00
Ni	0.00	0.00	0.00	0.00	0.00	0.00	0.00	0.00	0.00
Total	24.00	24.00	24.00	24.00	23.90	23.94	23.91	24.00	23.93
Cr #	0.63	0.64	0.68	0.64	0.64	0.61	0.63	0.63	0.63
Mg #	0.59	0.63	0.56	0.59	0.62	0.57	0.57	0.56	0.53
Al ratio	0.35	0.35	0.31	0.34	0.35	0.38	0.36	0.36	0.36
Fe^{3+} ratio	0.06	0.04	0.05	0.05	0.04	0.02	0.02	0.03	0.02
$100Cr/(Cr + Al + Fe^{3+})$	59.00	61.22	64.54	60.28	60.86	59.62	61.99	61.28	61.51
$100Mg/(Mg + Fe^{2+})$	59.39	63.43	55.60	58.52	62.26	57.02	57.38	56.34	52.98
$100Fe^{3+}/(Fe^{3+} + Cr + Al)$	5.77	3.96	4.66	5.40	4.19	2.28	1.71	2.70	2.14
$100Al/(Al + Fe^{3+} + Cr)$	35.21	34.81	30.79	34.30	34.94	38.08	36.28	36.01	36.33

4.1. Mafic-ultramafic rocks

Drilling has provided fresh samples from the complete stratigraphy. Primary igneous textures and minerals are largely preserved throughout the stratigraphy, but are extensively replaced by serpentine in most olivine-rich rocks. The mafic rocks commonly show major transformations due to the regional amphibolite to granulite-facies metamorphism. In the Ipueira and Medrado areas, the petrographic textures and chemical compositions of the main minerals of the mafic-ultramafic rocks were thoroughly studied (Marques and Ferreira Filho, 2003). Here, some aspects are highlighted and new petrographic information is added from all four studied segments.

The Jacurici Complex shows some distinct differences between the south and the north segments in terms of petrology and mineralogy. The Ultramafic Zone rocks of the segments in the southern part are predominantly composed of dunites, with minor harzburgites and rare orthopyroxenites, showing a predominance of olivine in most ultramafic rocks. Magmatic intercumulus amphibole (hornblende-tschermakite to Mg-hornblende) occurs in both LUU and UUU, but is more abundant in the UUU. The dunite shows typical adcumulate textures but is normally extensively serpentinized (Fig. 7A), while serpentinization in harzburgites is variable. Large oikocrysts of orthopyroxene with olivine inclusions are common and produce a mottled appearance on drill core surfaces. This texture is common in all segments. Orthopyroxene may also occur as rounded crystals with olivine (Fig. 7B). Clinopyroxene is rare, and magmatic colorless amphibole may occur in some layers, mainly in the UUU, as well as phlogopite, which is closely associated with chromite. On the other hand, the Ultramafic Zone rocks from the segments that outcrop to the north are comparatively enriched in pyroxene in the LUU and, especially, in the UUU. Clinopyroxene is relatively common in the ultramafic rocks from the northern part of the Complex. Lherzolite is present instead of harzburgite (Fig. 7C) in the LUU, which also contains a limited amount of magmatic amphibole. Pyroxenites are more common in the UUU in the northern part and occur as websterite (Fig. 7D) instead of orthopyroxenite or pyroxene-rich harzburgite, which is common in the southern part. Pyroxene-rich rocks may have major amounts of colorless magmatic amphibole. Regarding the mafic rocks, they are fine- to medium-grained mesocumulates, primarily represented by norite in the southern area (Fig. 7E) and gabbronorite in the northern part, with primary amphibole (Mg-hornblende) and phlogopite in variable amounts. When metamorphosed, the rocks show granoblastic textures and a mineral assemblage comprised of plagioclase, hornblende, biotite and rare garnet (amphibolite facies). The gabbroic rocks from the marginal zone (restricted to the southern part) are highly sheared and friable and show clinopyroxene and plagioclase that is strongly fractured (Fig. 7F).

The Várzea do Macaco segment experienced sulfidation during the crystallization and Ni-Cu-Fe sulfides (pyrrhotite + pentlandite + chalcopyrite) occur mainly in an interval with disseminated

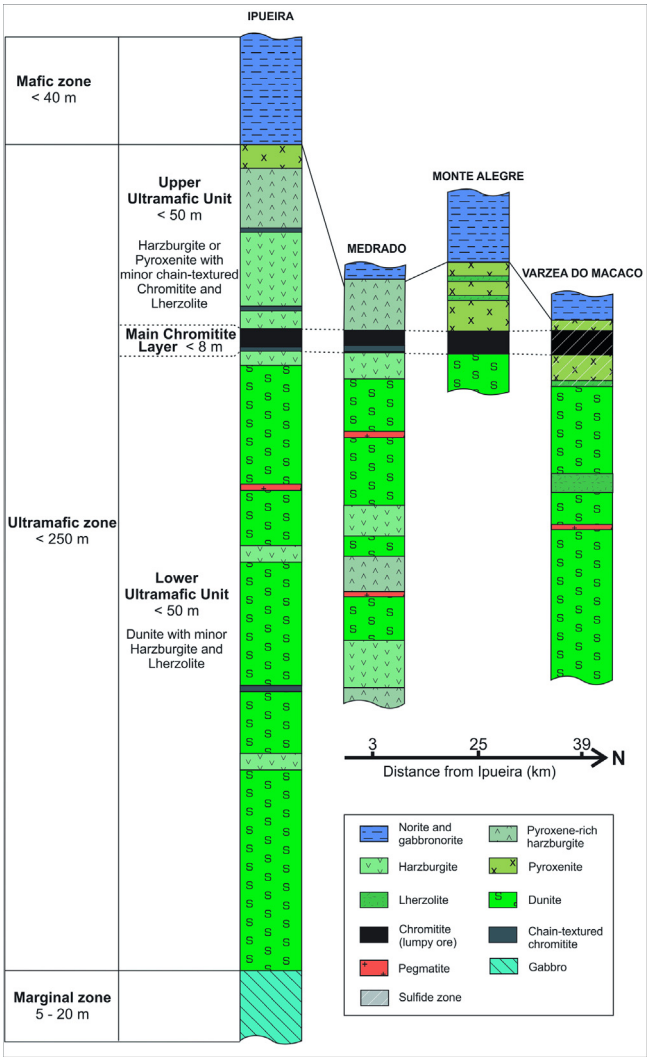

Fig. 3. Representative sections of the studied segments (Ipueira, Medrado, Monte Alegre Sul and Várzea do Macaco) showing stratigraphic correlation and the divisions suggested for the layered intrusion. An indication of the present distance between the segments towards north is indicated.

sulfides (1–15 vol.%) that starts in the LUU, 20 m below the MCL, and ends 15 m above the MCL in the UUU. No significant sulfidation was observed in the south, but a small amount of sulfides can occur at this stratigraphic level. Deformation is more intense in the northern segments compared to the Ipueira and Medrado segments. Large elongated grains of orthopyroxene and clinopyroxene were partially recrystallized into a fine-grained granoblastic orthopyroxene aggregate with no orientation, indicating a period of static recrystallization (Fig. 7G). Cumulate rocks become locally highly foliated, hampering the identification of magmatic textures and mineralogy throughout the stratigraphy. Secondary amphibole (green color in natural light) is more common and a secondary phlogopite is also abundant (Fig. 7H), revealing significant metasomatic intervals at the Várzea do Macaco, where a strong remobilization of the sulfides occurred. In all segments, the Jacurici Complex is crosscut by normal faults and shows many fault-related brittle structures, generally filled by alkaline pegmatites that are probably related to the Itiúba Syenite magmatism.

4.2. Chromitites

The Main Chromitite Layer varies from 5 to 8 m in thickness according to FERBASA internal reports, and except for a very discrete local increase of silicates (Fig. 8A), the MCL is a massive fine-grained cumulate with more than 90 vol.% of well-preserved chromite (Fig. 8B). Within each mafic-ultramafic segment, the MCL extends along strike for several meters interrupted only by normal faults. At Ipueira and Medrado, the chromitites were described by Marques and Ferreira Filho (2003). In the new sections from the recent drilling campaign, similar features were observed. Near the base of the MCL, a sub-layer of chain-textured chromitite occurs, which comprises 60–80 vol.% of small chromite grains surrounding larger serpentinized olivine or orthopyroxene grains (Fig. 8D, E). Chain-textured chromitite occasionally occurs as thin layers inside the LUU or UUU intervals, but exhibits less lateral continuity and shows variable thickness from a few centimeters up to 1 m. The hanging wall and footwall of the MCL and the thin chromitite seams are mainly harzburgites and, to a lesser extent, olivine orthopyroxenites. The contacts are commonly affected by later faults. When preserved, the contact between the MCL and its host rock is generally sharp and planar. Nevertheless, it was observed that the amount of chromite increases in the ultramafic rocks located immediately below the MCL. Occasionally, it is possible to observe that the contact between the chain-textured and the massive chromitite inside the MCL is slightly undulating (Fig. 8D).

Internally, the MCL is mainly composed of euhedral to subhedral chromite grains, varying in size from 0.1 to 0.8 mm (Fig. 8B). Silicates are rare and generally serpentinized or replaced by carbonate, talc or chlorite. Locally it is possible to identify orthopyroxene and minor amphibole. Olivine is rare. Large poikilitic silicates (up to 1.5 cm) were observed, normally consisting of partially or totally serpentinized orthopyroxene enclosing small (0.05–0.2 cm) chromite grains. Another recurrent texture in the MCL is massive chromite bands formed by many densely packed, poorly size-sorted chromite grains (Fig. 9A).

Chromite crystals often show dozens of tiny inclusions (being a few microns in diameter) with quite variable compositions, sizes and forms (Fig. 9B to H). SEM-EDS semi-quantitative analyses of the inclusions allowed the identification of olivine, orthopyroxene, amphibole (possibly Mg-hornblende), phlogopite, sulfides and Ti-rich oxides (Fig. 9). Some inclusions can be considered as being captured by chromite grains during growth or cooling and annealing, and form tracks that mark the euhedral pattern of the grain (Fig. 9B, E, F). In other circumstances, the inclusions occur all over the grain and can be considered to be trapped during crystallization (Fig. 9 C, D, G, H). Further studies are necessary to evaluate the inclusions.

Regarding the sulfide mineralization, the Ni, Cu and platinum group elements (PGE) grades are not disclosed under a confidentiality agreement. Sulfides show a primary stratigraphic control. They occur as disseminated and interstitial sulfides, associated with a ~20 m thick pyroxenite layer below the MCL and a pyroxene-rich harzburgite layer above the MCL in the Várzea do Macaco segment. Sulfides also occur in association with chromite, especially in the chain-textured ore, where sulfide (pyrrhotite + pentlandite) inclusions in chromite are common (Fig. 8C). The sulfide is predominantly comprised of pyrrhotite, with pentlandite and minor chalcopyrite. Massive sulfide lenses crosscut the pyroxenite and harzburgite layers at this stratigraphic level. These massive lenses are about 5 cm thick and are also composed of pyrrhotite, with pentlandite and minor chalcopyrite. Additionally, the deformation that took place in some layers remobilized the sulfide along the foliation and concentrated sulfides along small folds and veinlets, where it is associated with carbonate and serpentine. It is possible to recognize veins crosscutting the chromite layering (Fig. 8F). In the Ipueira and Medrado segments, where sulfidation is insignificant, Lord et al. (2004) reported that the highest total PGE concentrations were found exclusively in the chromitites, with

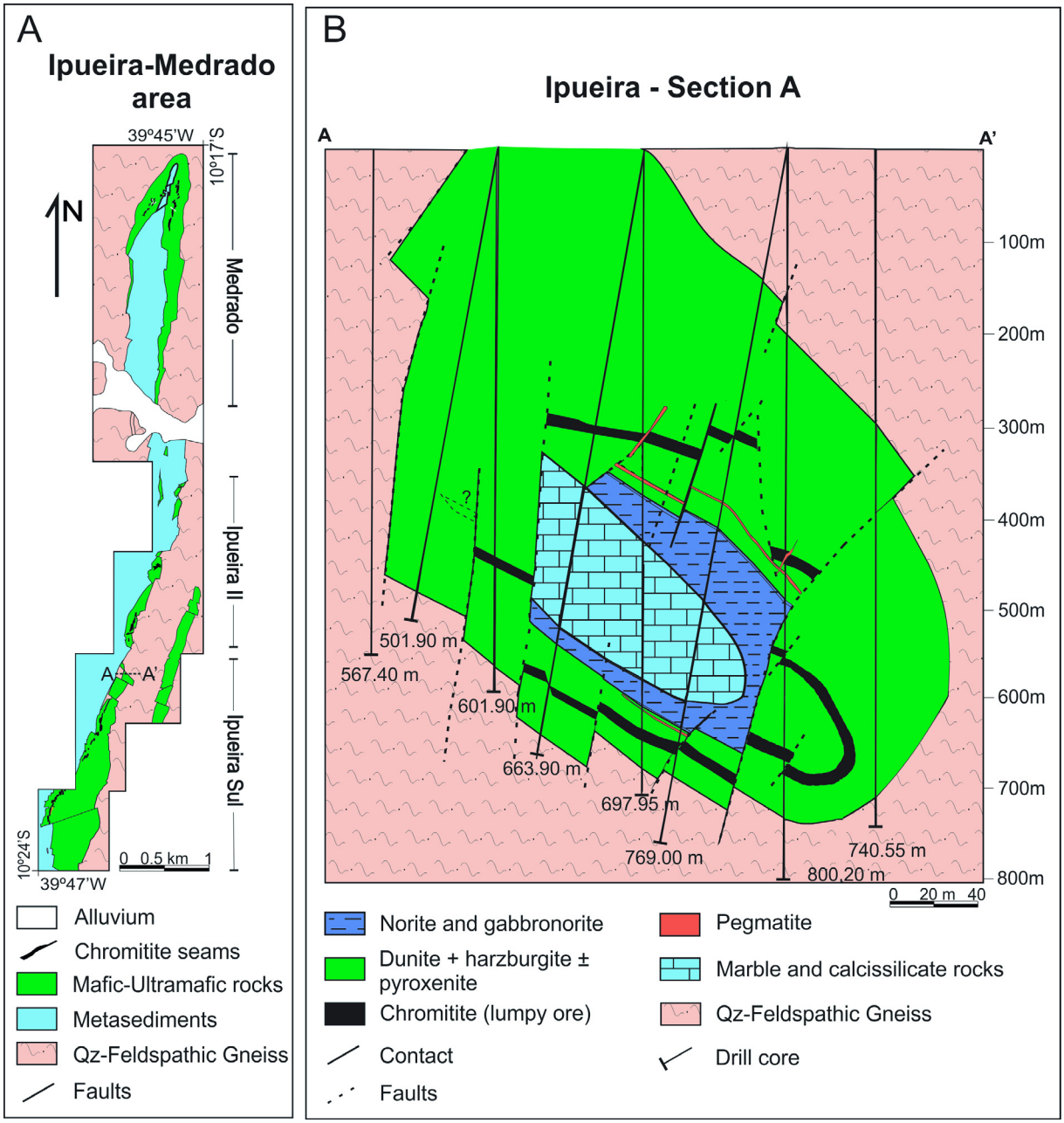

Fig. 4. A. Simplified geological map from the Ipueira and Medrado segments of the Jacurici Complex. B. Representative geological section of the Ipueira segment where underground mining is currently taking place. The section exemplifies the folded nature of the layered intrusion and the expressive thickness of the main chromitite layer. Adapted from FERBASA Geology Division, internal report.

results showing low (<350 ppb) amounts and unfractionated PGE patterns.

4.3. Composition of chromites

Compositional variations in chromite through the MCL from five drill cores, two from the Ipueira segment, one from the Medrado segment (data from Marques and Ferreira Filho, 2003), one from the Monte Alegre Sul and one from the Várzea do Macaco segments, are shown in Fig. 10. Note that the analyses of the chain-textured intervals show significant Fe-Mg drift due to trapped liquid shift effects (e.g. Roach et al., 1998) or sub-solidus exchanges with the silicates (e.g. Barnes and Jones, 2013; Eales and Reynolds, 1986; Irvine, 1965). The chromite from the chain-textured interval of the MCL shows less MgO and more FeO than the chromite from massive chromitites, producing a lower Mg number (molar Mg/[Mg + Fe^{2+}]) (Fig. 10 and Table 2). Regarding the Cr number (molar Cr/[Cr + Al]), it is lower when compared to results obtained from the massive layers. However, this is an effect of the trivalent exchange between Cr^{3+} and Fe^{3+}, rather than Cr^{3+} and Al^{3+}, as illustrated in Fig. 11C. The chromite from the chain-textured intervals are enriched in Fe_2O_3.

When considering only the intervals of chain-textured chromitites, it is clear that the composition varies less in the MCL (higher MgO and lower TiO_2), in comparison to chromitite seams from the LUU or UUU (Fig. 10, Fig. 11, Table 2). Considering only the chromite from the massive samples within the MCL in all segments, it is possible to observe a discrete increase of the Mg number from the base towards the middle of the layer, followed by a gradual decrease of the Mg number towards the top, except for one sample from the Monte Alegre Sul segment (Fig. 10). The Fe^{3+} ratio (molar Fe^{3+}/[Fe^{3+} + Al + Cr]) shows an opposite trend; this can be

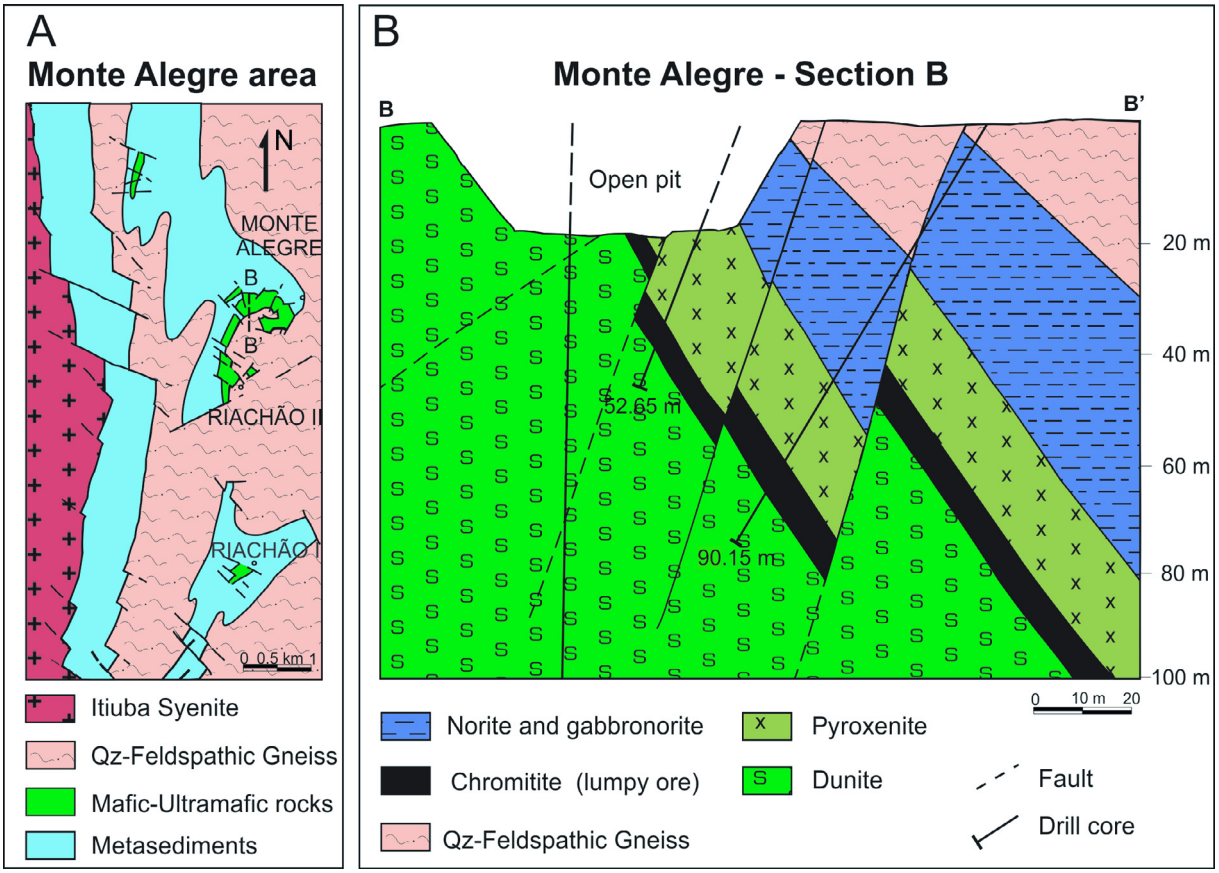

Fig. 5. A. Simplified geological map from the Monte Alegre Sul segment of the Jacurici Complex. Modified from Marinho et al. (1986). B. Representative geological section of the Monte Alegre Sul segment. Adapted from FERBASA Geology Division, internal report.

considered as a consistent pattern. Note that the MCL layer in the Ipueira II drill core is duplicated owing to a normal fault displacement (Fig. 10). Both intervals show the same compositional behavior and the Cr number does not vary significantly.

The chromites from the massive layers of all mineralized segments from the Jacurici Complex show a similar composition in comparison to other chromite-bearing layered deposits, such as those from the Bushveld Complex (Cameron, 1977, 1978; De Waal, 1975; Eales and Reynolds, 1986), the Stillwater Complex (Campbell and Murck, 1993) and the Great Dyke (Wilson, 1982), and also thick chromitites from the Kemi (Alapieti et al., 1989), Sukinda (Chakraborty and Chakraborty, 1984; Mondal et al., 2006, 2007) and Uitkomst (Yudovskaya et al., 2015) (Fig. 11D-F, Table 2), with a high Cr ratio and MgO and FeO exchanges in response to magma composition and fractionation. The TiO_2 level is low, possibly in response to a low Ti parental magma and a low degree of fractionation in the interval where the massive chromitites formed. The chain-texture chromitites from the UUU show higher TiO_2 levels, consistent with the higher degree of fractionation in this interval (Fig. 11B).

5. Discussion

5.1. Petrogenesis

The Jacurici Complex represents the remnants of voluminous magmatism, possibly the feeders and sub-chambers of a large igneous province. Previous studies of the Ipueira and Medrado segments considered them to be parts of a single intrusion that has acted as a sill-like conduit, where a huge volume of magma flowed through leaving behind peridotitic cumulate rocks and a 5–8 m thick MCL (Marques and Ferreira Filho, 2003). Many other segments located farther north, following a N-S trend, also host similar chromitite layers. In the Monte Alegre Sul and Várzea do Macaco segments, the thick chromitite occurs at an analogous stratigraphic level to the Ipueira and Medrado segments, and it is very possible that all segments were part of a single elongated intrusion which has been fragmented into several segments and displaced along a shear zone during the Paleoproterozoic.

The hypothesis that the sill acted as a conduit was conceived by considering that a magma column over 10 km thick would be necessary to form a 5–8 m thick massive chromitite (Marques and Ferreira Filho, 2003). In order to better understand the evolution of the magmatism, the compositional variation of olivine and orthopyroxene from dozens of harzburgite samples from different sections in the Ipueira and Medrado segments were studied by Marques and Ferreira Filho (2003). Two different magmatic regimes were identified in this study. The first interval, represented by the LUU, is typified by a slow upward increase in the Mg-ratio in olivine and orthopyroxene (Fo from 89.0 to 93.5, En from 88.0 to 94.5) (Fig. 12). The MgO enrichment peak is reached immediately below the thick chromitite layer (MCL) and it is considered an important marker in the evolution of the magmatic system. This first regime is assumed to be a response due to crystallization in a magmatic system, where repeated injections of fresh, very primitive magma entered the magma chamber while fractionated melt was transferred to shallower chambers. The second interval occurs after the MCL, in the UUU, where the behavior of the Mg-ratio in olivine and orthopyroxene is reversed and it is

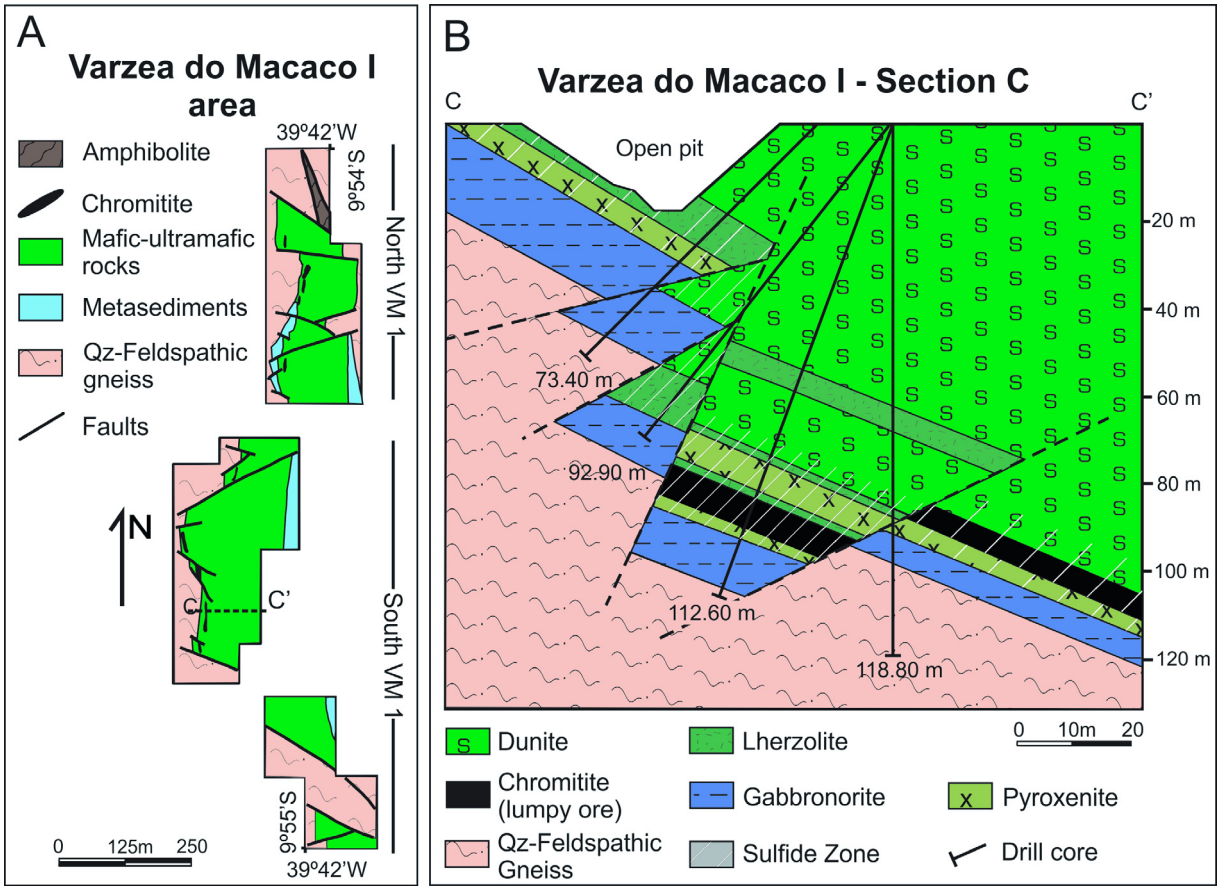

Fig. 6. A. Simplified geological map from the Várzea do Macaco segment of the Jacurici Complex. B. Representative geological section of the Várzea do Macaco segment. Adapted from FERBASA Geology Division, internal report.

characterized by a rapid upward decrease (Fo from 90 to 84, En from 90 to 82) (Fig. 12). The second regime is interpreted as the result of fractionation in the magmatic system, where insignificant injections of fresh magma occurred, allowing fractionation towards a more evolved composition, ending with crystallization of plagioclase and a mafic unit at the top of the intrusion.

The higher Mg number in the chromites from the MCL is considered to be a consequence of crystallization from a very primitive parental liquid. This is consistent with the results obtained from the harzburgite interval immediately below the MCL, which is the most undifferentiated, as indicated by the composition of olivine (Fo contents up to 93) and orthopyroxene (En contents up to 94). The discrete increase towards the middle of the MCL, with a decrease towards the top, is also consistent, showing that the magma evolved to an increasingly differentiated composition towards the top, which is observed in olivine and orthopyroxene of the harzburgites located above the MCL in the UUU (Fig. 12). When considering the chain-textured chromitites, the evolution of the magmatic system is even more evident. The chain textured chromitite within the MCL shows a less differentiated composition, which is compatible with the cryptic variation of the olivine and orthopyroxene from the harzburgites located at the top of the UUU. The more differentiated character observed in chain textured seams of the UUU interval, which shows a relatively lower Mg number and higher TiO_2 content (Fig. 11A, B), follows the fractionation pattern observed in silicates from the UUU.

Regarding the nature of the parental magma, Marques et al. (2003) performed a detailed study of the Ipueira and Medrado segments using trace elements and isotopes (Nd and Os). The rocks are characterized by high Zr, a high content of large ion lithophile elements (LILE) and light rare earth elements (LREE), and depleted Ta. The trace elements signature suggests that the parental magma of the mafic and ultramafic rocks was originally enriched in LILE, LREE and Zr and strongly depleted in Nb.

To compare the parental liquid of the MCL to the parental liquid of other chromitites, and to suggest a magma type, we followed the same procedures applied to massive chromitites from the Nuasahi and Sukinda Massifs by Mondal et al. (2006) using the equations proposed by Maurel and Maurel (1982) to calculate the Al_2O_3 content and FeO/MgO (wt.%) of the liquids in equilibrium with chromitite (for details, see Mondal et al., 2006). The results obtained for the MCL, considering the range of compositions in chromite from all segments, point to a parental liquid varying from 12.35 to 13.93 (wt.%) Al_2O_3, with a FeO/MgO (wt.%) ratio between 1 and 1.43 where most samples produce an FeO/MgO (wt.%) ratio between 1.03 and 1.08. The MCL parental liquid could be considered to be similar to a boninite or to a low-Ti siliceous high-Mg basalt, with high FeO/MgO ratios, showing some similarities to melts in equilibrium with other massive chromitites.

Marques et al. (2003) proposed an Archean subcontinental metasomatically enriched lithospheric mantle as the source of the magmatism to explain the trace element signatures, the negative ε_{Nd} (≤ -4) and subchondritic Os (≤ 0) results from harzburgite whole rock and chromite separates in the massive seams of the LUU and the basal interval of the MCL. The parental magma was considered to have resulted from a high degree of melting of a subcontinental metasomatized lithospheric mantle.

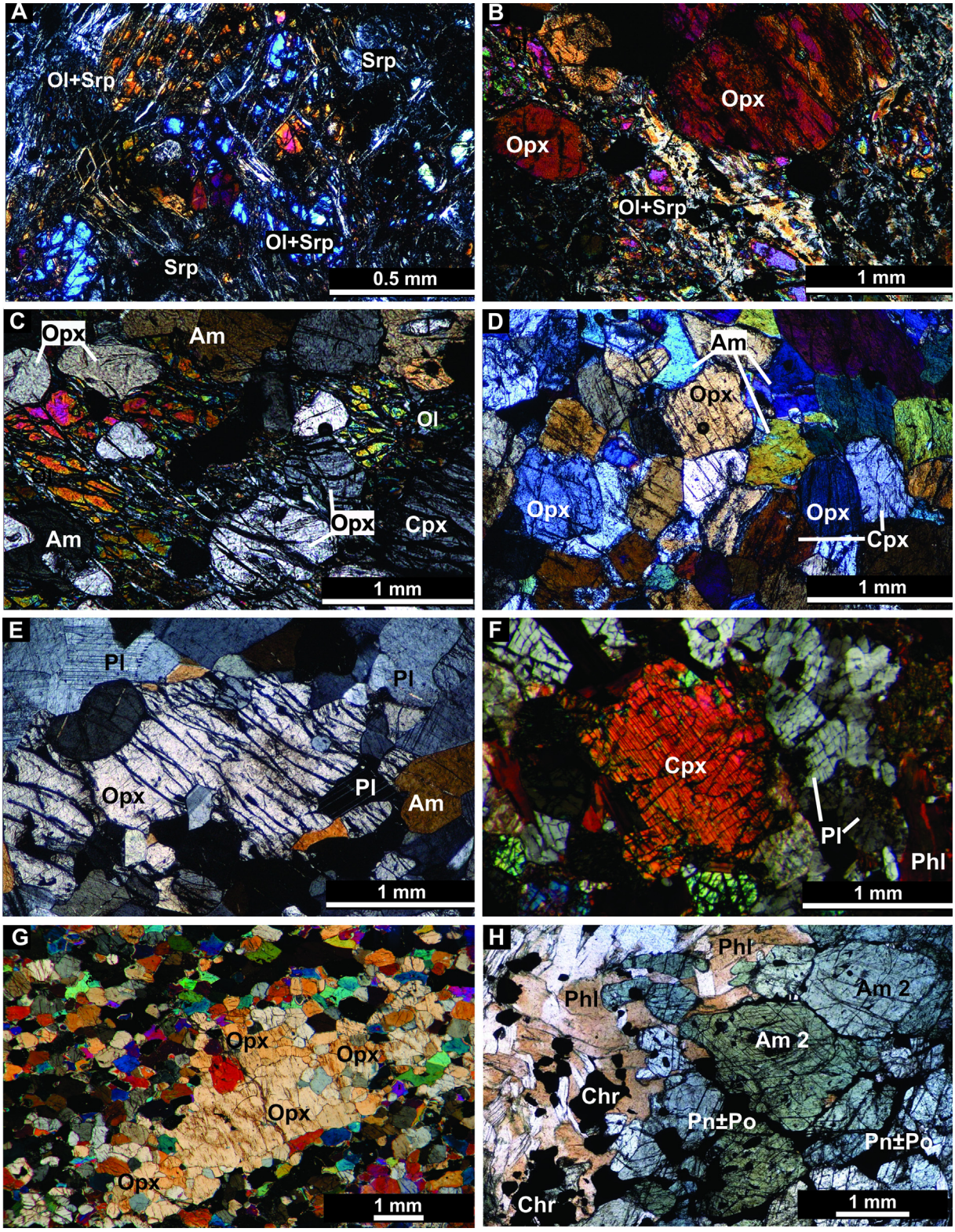

Fig. 7. Photomicrographs of representative rock types from the Jacurici Complex. A. Olivine adcumulate, partially serpentinized, from the LUU; B. Harzburgite showing rounded orthopyroxene and partially serpentinized olivine from the LUU; C. Lherzolite with rounded orthopyroxene and clinopyroxene and minor magmatic amphibole (colorless in natural light) from the LUU, northern Jacurici; D. Websterite, showing adcumulate texture with just a minor presence of magmatic amphibole, from the LUU, northern Jacurici; E. Norite orthocumulate with a small amount of amphibole (green in natural light – metamorphic?); F. Marginal gabbro showing a clinopyroxene and plagioclase that are strongly fractured; G. Large orthopyroxene crystal partially recrystallized into smaller orthopyroxene grains in a granoblastic texture; H. Amphibole associated with phlogopite and interstitial sulfides (Po + Pn) in a chromite-rich interval 1 m below the massive chromitite in a late metasomatic alteration zone, Várzea do Macaco segment.

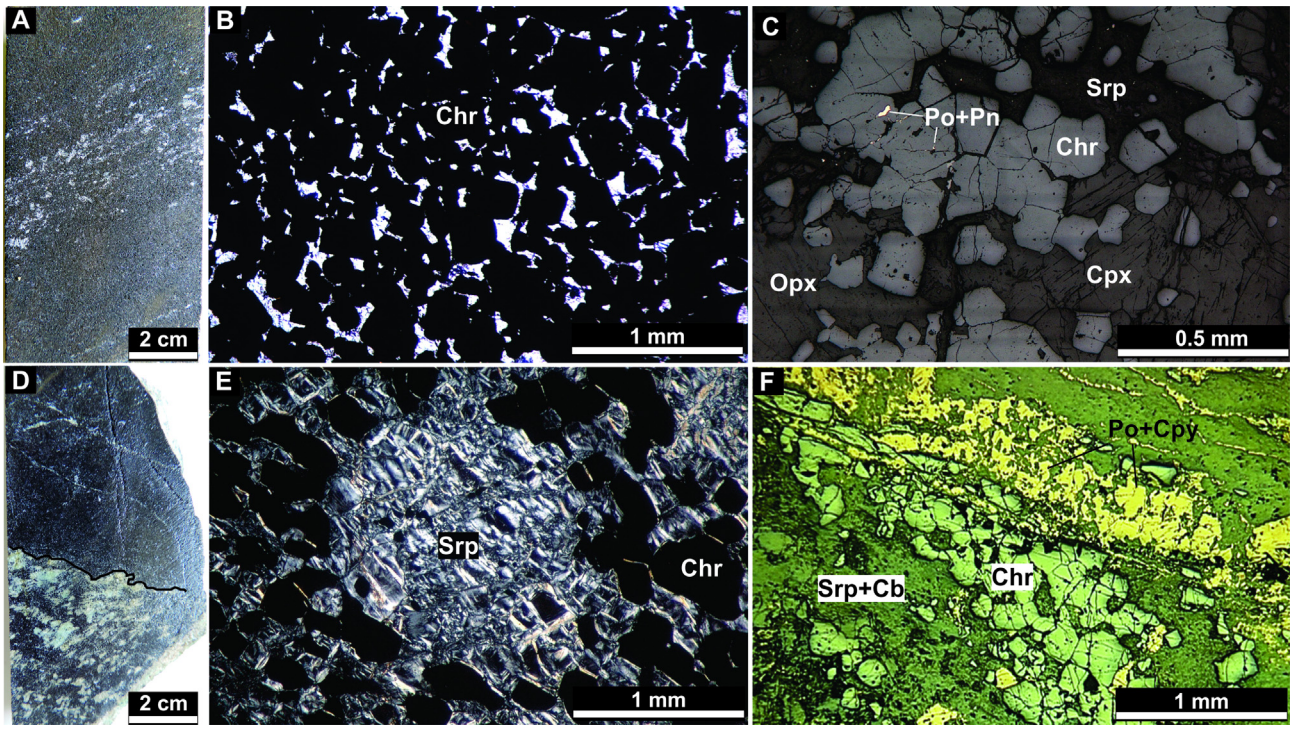

Fig. 8. Photographs and photomicrographs of chromitite textures. A. Photograph of a half core showing thin intervals enriched in silicates inside a very massive and fine-grained chromitite from the MCL; B. Massive chromitite showing euhedral to subhedral chromite grains; C. Inclusions of pyrrhotite and pentlandite in chromite grains from an interval of chromitite enriched in silicates (both orthopyroxene and clinopyroxene). MCL from the Várzea do Macaco segment; D. Photograph of a half core showing the contact between chain-textured chromitite and massive chromitite near the base of the MCL. Note the undulating nature of the contact. E. Chain-textured, fine-grained chromite surrounding (serpentinized) olivine or orthopyroxene grains; F. Chromitite thin layer intercepted by a sulfide-rich veinlet related to a late remobilization process. Chr – chromite, Opx – orthopyroxene, Cpx – clinopyroxene, Srp – serpentine, Po – pyrrhotite, Pn – pentlandite, Cpy – chalcopyrite, Cb – carbonate.

Marques et al. (2003) suggested crustal contamination in the MCL interval and above, based on the decline in ε_{Nd} and an increase in γ_{Os} towards the top. Chromitites show more radiogenic Os signatures and have positive γ_{Os} (up to 3.3) in the horizons immediately above the MCL (Fig. 12). An increasingly negative range of ε_{Nd} (≤ -6) is observed in rocks from the UUU which is coincident with an increase in magmatic amphibole content over that interval (Fig. 12). The presence of hydrous silicate phases as inclusions in chromite from chromitites, and an increase of amphibole near the MCL and toward the top of the intrusion are important features that suggest the magma was hydrated in those intervals. If the hydration is a result of crustal contamination, which is possible considering the isotope results, and whether or not that occurred at the site of the intrusion are issues that remain to be investigated.

In relation to other regional mafic-ultramafic intrusions, another chromium mineralized complex, the Campo Formoso Intrusion, occurs just a few kilometers to the west. Lord et al. (2004) tentatively correlated the Campo Formoso Intrusion with the Jacurici Complex. However, the ages are not well constrained, the regional geology is poorly understood and the fractionation and the mineralization show distinct paths and styles. It is reasonable to assume that the intrusions are not directly related, but it is possible that the underlying reservoir could have been the same, perhaps periodically producing chromium-enriched magma. A similar situation occurred in southern Africa where many deposits occur within a restricted area, and a common Cr-enriched source reservoir has been considered a possibility (Stowe, 1994).

5.2. Formation of the thick chromitite from the Jacurici Complex

Since the 1960's, several models have been proposed to explain the formation of chromitites in layered intrusions (Cameron, 1977; Eales, 2000; Irvine, 1975, 1977; Lipin, 1993; Maier and Barnes, 2008; Maier et al., 2013; McDonald, 1965; Mondal and Mathez, 2007; Naldrett et al., 2012; Sharpe and Irvine, 1983; Ulmer, 1969; Voordouw et al., 2009). Nevertheless, the geological mechanism that could promote the formation of massive layers of chromitite remains poorly understood.

The formation of the thick MCL in a thin intrusion in the Jacurici Complex is even more complicated to explain, especially when considering mass balance and lack of enormous amount of magma. The intrusion is assumed to have acted as a conduit, but the mechanism to form the massive layer is not well constrained. Marques et al. (2003) considered it difficult to explain MCL formation based upon magma mixing model (e.g. Campbell and Murck, 1993; Irvine, 1977), which involve new influxes of primitive melt entering into a magma chamber and mixing with a fractionated resident magma. The thick chromitite is located in an interval where the melt in the magma chamber reached its most primitive composition. It is followed by a more fractionated interval, the opposite to what would be expected from mixing model. Based on geochemical and petrographic evidence, the trigger for the chromite crystallization was considered to be crustal contamination (Marques et al., 2003). The more radiogenic Nd and Os isotope composition towards the top of the MCL and in the layers overlying the MCL, and the direct relationship between the more radiogenic composition and the modal increase in hydrous phases (amphibole) in harzburgites, were considered key features (Fig. 12). Ferreira Filho and Araujo, 2009 proposed that carbonate-bearing country rocks were assimilated, increasing the oxygen fugacity and triggering chromite crystallization. The sulfidation observed in the Várzea do Macaco segment, at the same level of the MCL, could also point to crustal contamination at this specific interval, but no detailed sulfide studies have been performed to confirm a crustal contribution. Contamination as a trigger to chromite

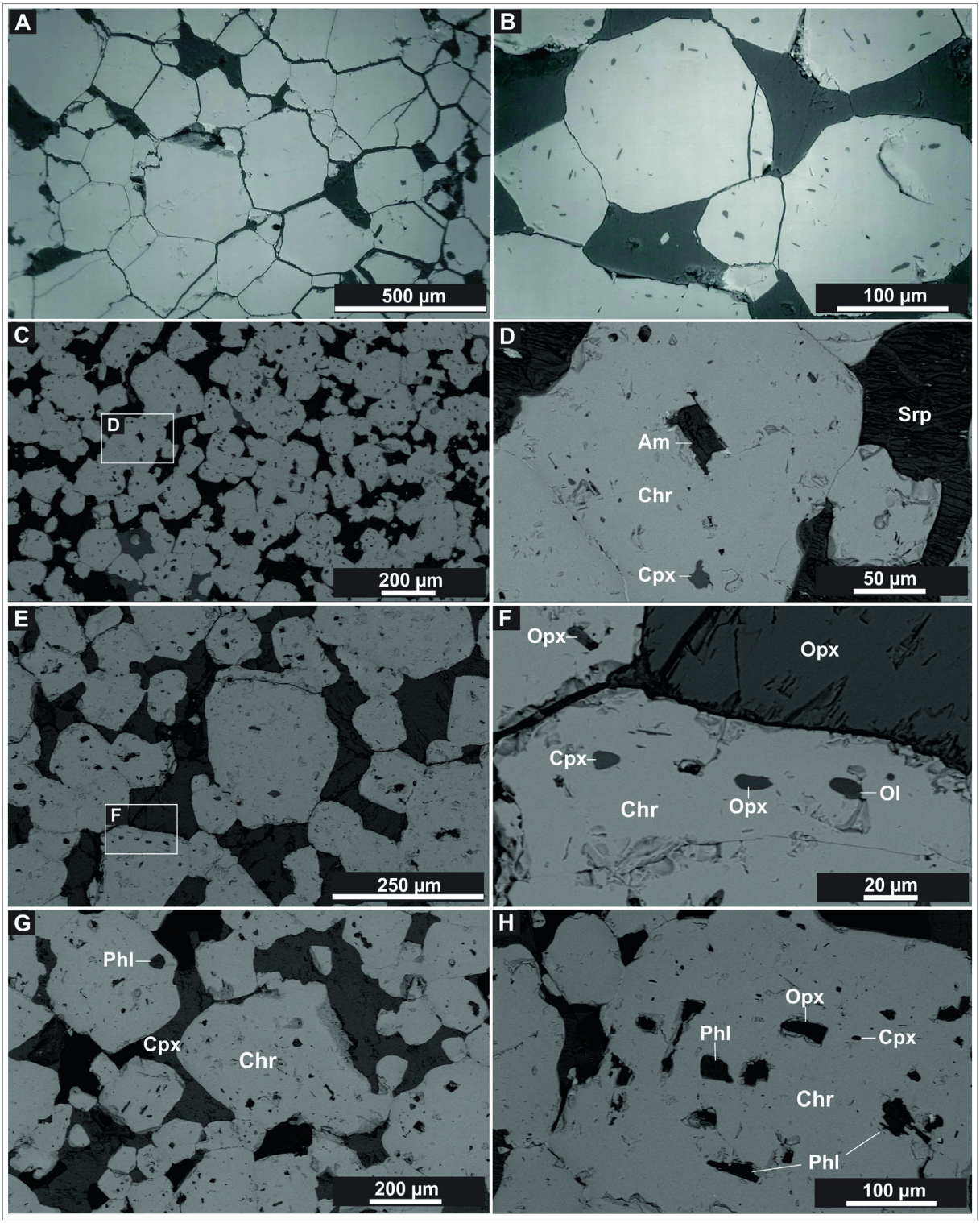

Fig. 9. Back scattered electron (BSE) images showing the textures and mineral assemblages of inclusions in chromites from the MCL. A. Overall aspect of massive chromitite showing densely packed poor size-sorted chromite grains with almost no inclusions. B: Silicate inclusions forming rings in chromite grains recording entrapment during chromite growth or annealing. C and E. Overall aspect of the massive chromitite with dozens of silicate inclusions randomly oriented. D: Detail of C showing polygonal amphibole and clinopyroxene inclusions. F. Detail of E, showing orthopyroxene, clinopyroxene and olivine oval-like shaped inclusions. G and H. chromites with large phlogopite and orthopyroxene polygonal inclusions and small clinopyroxene inclusions. Chr – chromite, Opx – orthopyroxene, Cpx – clinopyroxene, Ol– olivine, Am – amphibole, Phl – phlogopite, Srp – serpentine.

crystallization had been proposed by Irvine (1975), however Irvine (1977) abandoned this suggestion, considering the large amount of assimilation that was required to be unreasonable. Alapieti et al. (1989), Kinnaird et al. (2002), Rollinson (1997) and Spandler et al. (2005) all reconsidered crustal contamination in their studies. However, Mondal and Mathez (2007) and Naldrett et al. (2012)

argued against this mechanism based on thermodynamic modeling of the Bushveld Complex.

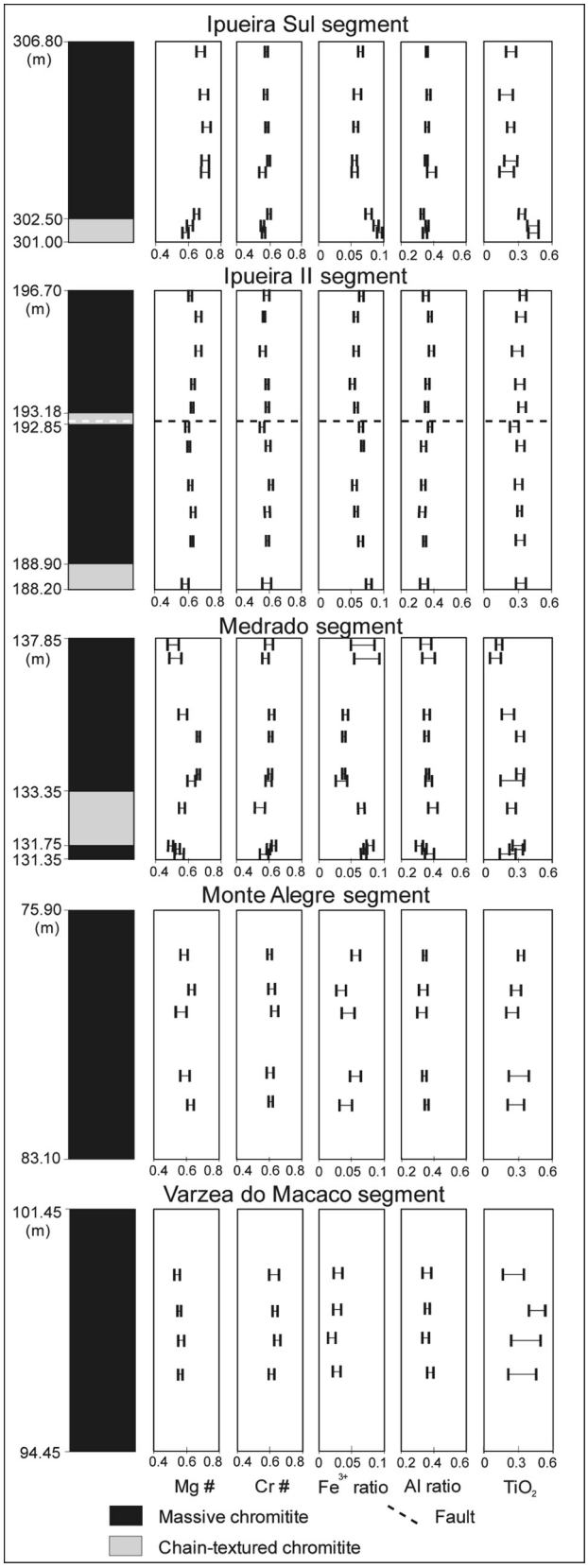

In the detailed petrographic study of the chromitites from the four segments, we found dozens of hydrous silicate minerals occurring as inclusions in the chromite. This feature, and the presence of amphibole as an important silicate phase in cumulate rocks adjacent to the MCL interval, is strong evidence that the parental magma could have been hydrated at the time of chromite crystallization. The more radiogenic isotope signatures reported by Marques et al. (2003) may be linked to the introduction of fluids in the magmatic system. The precise site where the magma was hydrated is difficult to determine, although it is possible to assume that water and other fluids could migrate from the country rock towards the conduit-shaped intrusion. Hydrous silicate inclusions in chromite are relatively common in ophiolite chromitite (e.g. Augé, 1987; Lorand and Ceuleneer, 1989; Melcher et al., 1997) and have also been described in stratiform chromitites (e.g. Jackson, 1961; Irvine, 1975; Li et al., 2005; Spandler et al., 2005). In investigating the Nuasahi and Sukinda Massifs, Mondal et al. (2006) suggested that a boninitic magma mixing with water-bearing magma derived from a supra-subduction setting could possibly explain the formation of the chromitites by suppression of silicate crystallization. In this case no crustal contamination had occurred, as indicated by non-radiogenic Os signatures in chromite (Mondal et al., 2007). The addition of fluids could also cause an increase in pressure, another mechanism that has been considered as a possible explanation for massive chromitite formation (Cameron, 1980; Lipin, 1993). On the other hand, Mondal and Mathez (2007) and Naldrett et al. (2012) considered the addition of water to be an unfeasible process to explain the Bushveld chromitites.

Alternatively, other mechanisms for chromitite formation have been proposed such as chromite slurries (Eales, 2000; Mondal and Mathez, 2007; Voordouw et al., 2009) or slumping of semi-consolidated cumulates causing layering and thickening (Maier and Barnes, 2008; Maier et al., 2013). The core idea of the chromite slurry model considers an intrusion of a batch of magma carrying previously crystallized chromite grains (Eales, 2000; Mondal and Mathez, 2007). Voordouw et al. (2009) suggested up to 60 vol.% chromite mush, with fluids helping to reduce viscosity. Regarding sliding of the cumulates towards the center of the chamber, Maier and Barnes (2008) and Maier et al. (2013) proposed that during subsidence of an intrusion, slumps of semi-consolidated cumulate, with cumulate unmixing, could have occurred in the middle and deeper parts of the chamber, with progressive thickening and sorting. Recently, Forien et al. (2015) performed experiments to investigate whether slumping of semi-consolidated cumulates could account for mineral layering and the formation of chromite layered deposits. Low angle inclination produced elongated thin deposits with uniform thicknesses, similar to what is observed in the Bushveld Complex, while higher angle inclination generated thicker deposits concentrated over a short distance. Maier et al. (2013) concluded that feeder conduits could concentrate dense minerals and dense slurries could sink back into the feeders.

The mineralized intrusion of the Jacurici Complex is here considered to be a conduit. The chromite composition from chromitites throughout the stratigraphy records a greater differentiation in composition towards the top, with the most primitive

Fig. 10. Stratigraphic variation of chromite compositions from chromitite samples throughout the Main Chromitite Layer from the Ipueira (Sul and II) segment (drill cores I-328-55 and I-306-75), the Medrado segment (drill core SSM-28-16), the Monte Alegre Sul segment (drill core MAS-105-65) and Várzea do Macaco segment (drill core VM1-88-70). Each data bar represents six to eight spot analyses. Mg# = 100Mg/Mg + Fe^{2+}. Cr# = 100Cr/Cr + Al. Fe^{3+} ratio = 100Fe^{3+}/Fe^{3+} + Cr + Al, Al ratio = (100Al/Al + Cr + Fe^{3+}).

Table 2
Main chemical features of olivine and chromite from chromite-mineralized layered complexes.

Layered Intrusion	Olivine composition		Chromite composition						
	Fo	Ni (ppm)	Unit	Texture	Cr #	Mg #	Al ratio	Fe^{3+} ratio	TiO_2
Ipueira[1]	84–93	1800–4700	MCL	Massive	0.60–0.68	0.56–0.72	0.31–0.41	0.04–0.09	0.14–0.49
			MCL	Chain textured	0.52–0.62	0.57–0.60	0.31–0.36	0.04–0.11	0.19–0.49
			UUU	Chain textured	0.44–0.56	0.44–0.52	0.35–0.49	0.11–0.19	0.30–0.75
			LUU	Chain textured	0.53–0.58	0.49–0.55	0.35–0.39	0.11–0.14	0.27–0.45
Medrado[1]	84–93	1800–4700	MCL	Massive	0.60–0.68	0.48–0.66	0.29–0.41	0.03–0.08	0.12–0.34
			MCL	Chain textured	0.57–0.63	0.51–0.57	0.33–0.39	0.05–0.08	0.14–0.29
Monte Alegre	n.a.	n.a.	MCL	Massive	0.62–0.68	0.53–0.64	0.30–0.35	0.02–0.06	0.19–0.53
Várzea do Macaco	n.a.	n.a.	MCL	Massive	0.59–0.65	0.52–0.58	0.33–0.39	0.01.–0.03	0.17–0.55
Bushveld[2]	83–88	1800–2200	LCZ, UCZ		0.55–0.74	0.30–0.65	0.20–0.35	0.04–0.13	0.65–1.81
Great Dyke[3]	84–92	1400–3500			0.52–0.78	0.23–0.69	0.19–0.37	0.01–0.24	0.23–1.65
Stillwater[4]	85–87	2100–2600	G, H		0.55–0.61	0.55–0.60	0.32–0.42	0.06–0.10	n.a.
Kemi[5]	82–83	n.a.			0.58–0.68	0.12–0.62	0.27–0.38	0.06–0.12	0.40–1.50
Uitkomst[6]	82–91	1700–4400			0.63–0.75	0.38–0.57	0.20–0.28	0.04–0.09	0.36–1.09
Nuasahi-Sukinda[7]	90–94	2100–4000			0.78–0.87	0.62–0.82	0.13–0.22	0.01–0.02	0.12–0.26

Cr # = Cr/(Cr + Al), Mg # = Mg/(Mg + Fe^{+2}), Al ratio = Al/(Al + Cr + Fe^{3+}), Fe^{3+} ratio = Fe^{3+}/(Fe^{3+}Al + Cr).
Abbreviations: Fo = forsterite; n.a. = not available; MCL = Main Chromitite Layer; UUU = Upper Ultramafic Unit; LUU = Lower Ultramafic Unit; UCZ = Upper Critical Zone; LCZ = Lower Critical Zone.

[1] Marques and Ferreira Filho (2003);
[2] Cameron (1977, 1978), De Waal (1975), Eales and Reynolds (1986);
[3] Wilson (1982);
[4] Campbell and Murck (1993);
[5] Alapieti et al. (1989);
[6] Yudovskaya et al. (2015);
[7] Mondal et al. (2002), Mondal et al. (2006).

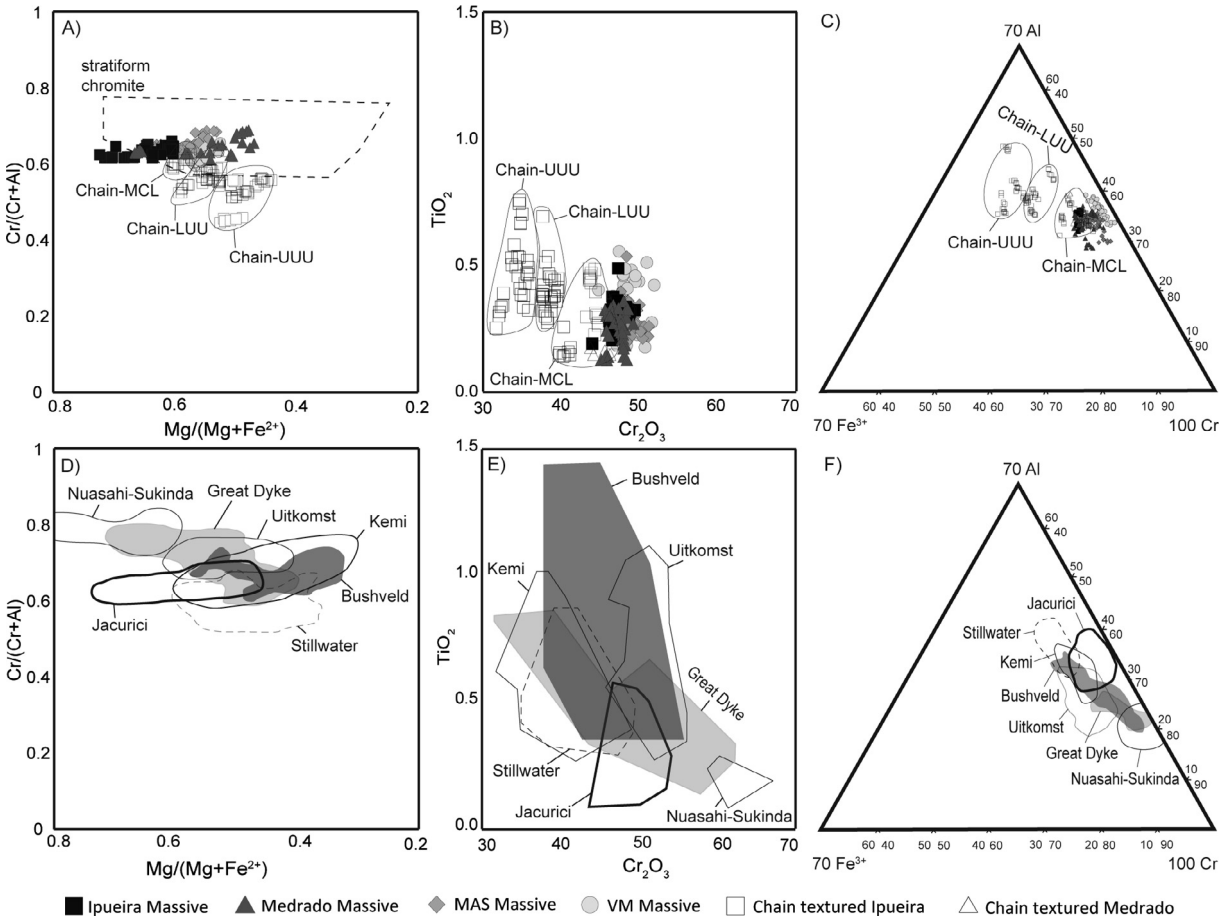

Fig. 11. Compositional variation diagrams from Jacurici Complex chromitites. Massive and chain-textured chromite compositions are plotted in A, B and C. Compositional fields of massive chromitites from the Jacurici Complex compared to other layered intrusions in D, E and F. Approximately 300 analyses are represented. Stratiform fields in (A) from Irvine (1967). Data for Great Dyke after Wilson (1982). Bushveld fields from Naldrett et al. (2009). Stillwater fields from Campbell and Murck (1993). Kemi fields from Alapieti et al. (1989). Uitkomst data from Yudovskaya et al. (2015). Nuasahi-Sukinda fields from Mondal et al. (2006) and Mondal (2009).

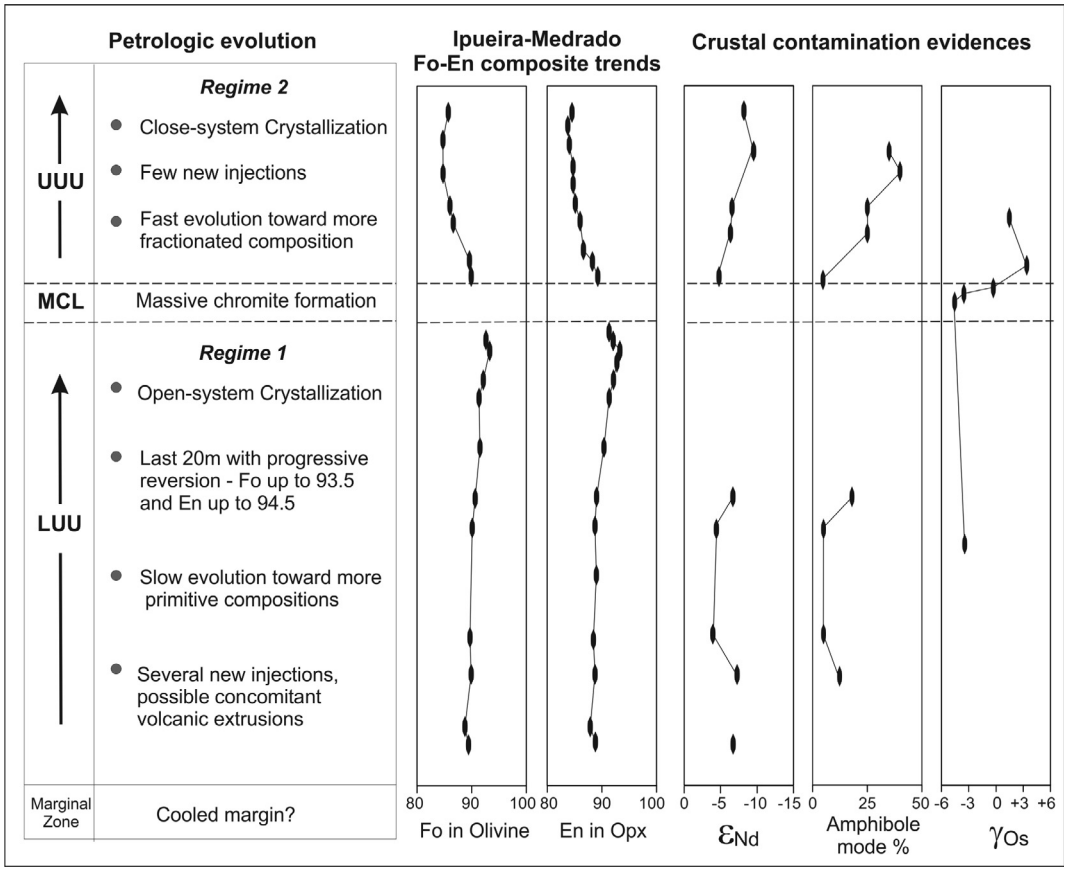

Fig. 12. Schematic petrologic evolution suggested for the mineralized Jacurici complex intrusion based on up-stratigraphy variation in olivine and orthopyroxene composition, petrography and Nd (whole rock) and Os (chromite separates) isotope composition (data from Marques and Ferreira Filho, 2003 and Marques et al., 2003).

composition reached at the base of the MCL in all studied segments, absolutely coherent with the trends observed in the silicate rocks. It suggests that the chromite crystallized from liquid that was flowing through the magma chamber. In this scenario, magma, laden with previously crystallized chromite grains, would be difficult to reconcile. Here we propose a model (Fig. 13), following the main suggestions of Maier et al. (2013), considering chromite-rich feeder conduits. A summary of the idea follows:

1. A very primitive magma started to be extracted from a possible Cr-enriched subcontinental metasomatized lithospheric mantle. It ascended through a regional structural pathway that controlled the conduit.
2. The conduit was slightly enlarged deep in the crust, in an area proximal to the contact between a quartz-feldspathic granite-gneiss-migmatitic basement and a metamorphosed sedimentary sequence containing marbles and calc-silicate rocks. Cumulate olivine-rich rocks crystallized during a stage where the conduit-shaped magma chamber was continuously replenished with primitive magma influxes.
3. The primitive composition of the magma reached its maximum MgO to FeO ratio, producing crystals of olivine with Fo up to 93.5 and orthopyroxene with an En of up to 94.5 at the top of LUU. The hottest magma was possibly contaminated with fluids from the country rocks. Hydration of the magma is recognized by the presence of amphibole in harzburgite close to this interval, and by the many inclusions of hydrous silicate minerals in chromite from the MCL. The contamination is inferred from the isotope results. The addition of fluid, increase in pressure, and/or contamination, could have favored the crystallization of chromite. However, as discussed before, there is no consensus on the role of fluids, pressure or contamination concerning chromitite formation.
4. Independent of the mechanism that could have triggered the chromite crystallization, we suggest that chromite may have accumulated along the margins of the conduit in response to the magma flow, forming a slurry with semi-consolidated chromite. A similar idea is proposed in the model of Voordouw et al. (2009). Recently, Chistyakova et al. (2015) documented chromite forming on the walls of conduits, and suggested that deeper chromite-rich conduits could exist below magma chambers. Concentration of chromite on the walls is attributed to the very efficient removal of differentiated melt along the magma flow pathway (Chistyakova et al., 2015).
5. The presence of fluids may have promoted slumps of a chromite-rich slurry. The chromite-rich mush from the walls of the conduit slumped and accumulated to form a thick chromitite with a mixture of different grain sizes that were later compacted (Fig. 8B and D). Although the original slope of the conduit walls is unknown, we speculate a moderate angle considering the thickness and limited lateral extension of the chromitite, according to the results of the experiments from Forien et al. (2015). The current may have eroded part of the previously deposited cumulate silicate layer from the magma chamber, causing the sharp contacts observed between the MCL and LUU. The remaining intercumulus liquid ascended from the mush (cf. Eales, 2000) leaving behind a very pure chromitite. In the north part of the chamber, sulfidation possibly occurred at that moment, forming sulfides that percolated throughout the chromitite and its footwall rocks, thereby forming a disseminated Ni-rich and Cu ore.

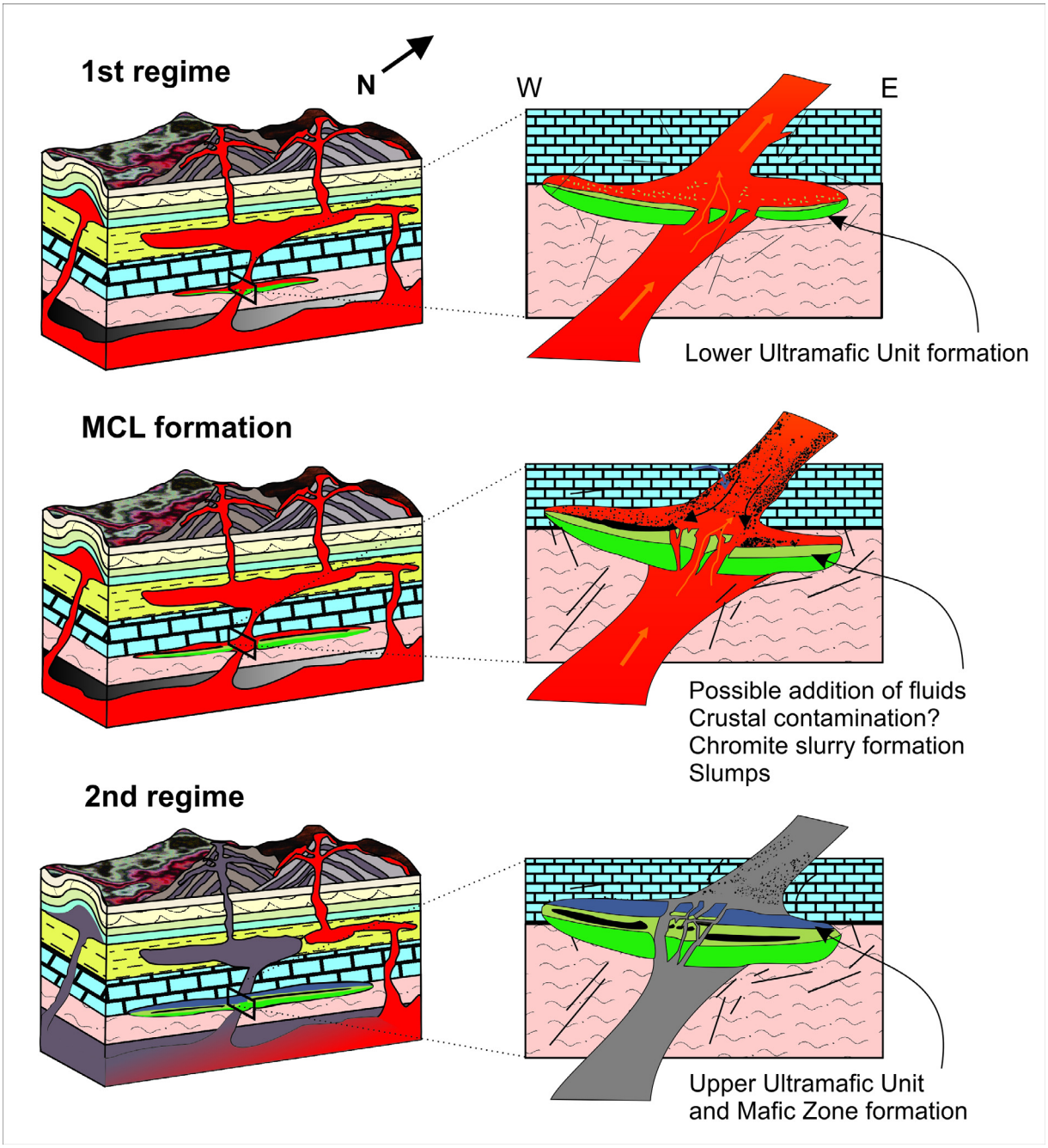

Fig. 13. Schematic diagram illustrating the formation of the chromite deposit of the Jacurici Complex considering a conduit-shaped chamber. The chromite crystallized in situ along the margins of the conduit creating a semi-consolidated chromite slurry that slumped and formed a thick chromitite inside the enlarged part of the chamber where layered ultramafic rocks were previously formed. Afterwards, the conduit was obstructed and the resident magma fractionated and crystallized producing more evolved rocks.

6. The conduit was gradually obstructed and the resident magma fractionated, crystallizing differentiated silicates and chromite. In the latest stages, cumulus plagioclase crystallized, forming the gabbronorites of the Mafic Unit at the top of the intrusion.

6. Conclusions

1. The Jacurici Complex represents the remnants of voluminous magmatism, possibly the feeders and sub-chambers of a large igneous province.
2. The mineralized segments of the complex present a similar stratigraphic succession, with a thick chromitite (MCL) occurring at an analogous interval in each segment. They are considered to be part of a single N-S elongated intrusion that was fragmented into several segments and displaced along a shear zone during the Paleoproterozoic.
3. The parental magma was previously considered to have been derived from a subcontinental metasomatized lithospheric mantle (Marques et al., 2003) and its Al_2O_3 and FeO/MgO composition was estimated to be equivalent to that expected from a

boninite or, alternatively, a low-Ti, siliceous, high-Mg basalt with higher FeO/MgO.

4. The Jacurici Complex intrusion is assumed to have acted as a conduit, as previously suggested by Marques and Ferreira Filho (2003) to explain the formation of a thick chromitite within a thin layered intrusion.
5. Detailed petrography of samples from all segments of the MCL chromitite revealed hydrous silicate minerals as common inclusions. This feature and the abundant presence of amphibole in the interval adjacent to MCL suggest that the magma was hydrated during chromite crystallization. The crustal contribution observed in isotope results (Marques et al., 2003) may be related to the addition of fluids into the melt, perhaps at the site of the intrusion.
6. The chromite composition records a different composition towards the top, following the silicate behavior, with the most primitive composition at the base of the MCL in all studied segments. Chromite probably crystallized directly from the liquid that was flowing through the magma chamber.
7. Crustal contamination has been considered (Marques et al., 2003; Ferreira Filho and Araujo, 2009) as the mechanism to crystallize chromite in a single phase. However, the trigger for chromite crystallization is debatable. Fluids may have played an important role, but it remains an open question.
8. The crystallization and accumulation of chromite is suggested to have occurred along the walls of the conduit, forming a slurry, which slumped and was concentrated in the magma chamber forming a massive thick chromitite layer after the remnant liquid ascended from the mush. The presence of fluids may have helped in mobilizing the slumps.

Acknowledgements

Companhia de Ferro Ligas da Bahia (FERBASA) and its staff are gratefully acknowledged for field support, geological information and allowing sampling of the drill cores. JRVPD and BF acknowledge the Programa de Pós-Graduação em Geociências da Universidade Federal do Rio Grande do Sul – Brazil and the Conselho Nacional de Desenvolvimento Científico e Tecnológico – Brazil (CNPq) for their scholarships. We are grateful to Isadora Henrichs and Adam D. McArthur for their time reviewing the manuscript. We thank the graduate student Gabriel Bertolini and the undergraduate students Vinícius M. Peixoto, Natanael M. Cezario and Renan G. de Souza for their technical support and also acknowledge the microprobe laboratory staff from the Universidade de Brasília. César F. Ferreira Filho and Ahmed Hassan are thanked for their constructive comments that led to significant improvement of the manuscript. The guest editor, Sisir K. Mondal, is thanked for encouraging the submission of this manuscript and for his relevant comments and suggestions.

Appendix A. Supplementary data

Supplementary data associated with this article can be found, in the online version, at http://dx.doi.org/10.1016/j.oregeorev.2017.04.033.

References

Alapieti, T.T., Kujanpää, J., Lahtinen, J.J., Papunen, H., 1989. The Kemi stratiform chromitite deposit, northern Finland. Econ. Geol. 84, 1057–1077.
Almeida, F.F.M., Brito Neves, B.B., Carneiro, C.D.R., 2000. The origin and evolution of the South American platform. Earth-Sci. Rev. 50, 77–111.
Almeida, F.F.M., 1977. O cráton do São Francisco. Rev. Bras. Geocienc. 7, 349–364.
Augé, T., 1987. Chromite deposits in the northern Oman ophiolite: mineralogical constraints. Mineral. Deposita 22, 1–10.
Barbosa, J.S.F., Dominguez, J.M.L., 1996. Texto Explicativo para o Mapa Geológico da Bahia ao Milionésimo, ed. SICM/SGM, Salvador, Bahia, Brasil, 1–382.
Barbosa, J.S.F., Mascarenhas, S.J.F., Correa Gomes, L.C., Dominguez, J.M.L., Souza, J.S., 2012. Geologia da Bahia: Pesquisa e Atualização, ed. CBPM, Salvador, Bahia, Brasil 1, 1–559.
Barbosa, J.S.F., Sabaté, P., 2002. Geological features and the Paleoproterozoic collision of four Archean crustal segments of the São Francisco Cráton, Bahia, Brazil: a synthesis. An. Acad. Bras. Cienc. 74 (2), 343–359.
Barbosa, J.S.F., Sabaté, P., 2003. Colagem Paleoproterozoica de placas arqueanas do Cráton do São Francisco. Rev. Bras. Geocienc. 33 (1-Suplemento), 7–14.
Barbosa, J.S.F., Sabaté, P., Marinho, M.M., 2003. O Cráton do São Francisco na Bahia: Uma síntese. Rev. Bras. Geocienc. (1-Suplemento), 3–6
Barnes, S., Jones, S., 2013. Deformed chromitite layers in the coobina intrusion, Pilbara Craton, Western Australia. Econ. Geol. 108, 337–354.
Barnes, S.J., Roeder, P.L., 2001. The range of spinel compositions in terrestrial mafic and ultramafic rocks. J. Petrol. 42, 2279–2302.
Bastos Leal, L.R., Teixeira, W., Piccirillo, E.M., Leal, A.B.M., Girardi, V.A.V., 1994. Geocronologia Rb/Sr e K/Ar do enxame de diques máficos de Uauá, Bahia (Brasil). Geochim. Bras. 8, 99–114.
Brito Neves, B.B., Cordani, U.G., Torquato, J.R.F., 1980. Evolução geocronológica do Pré-cambriano do Estado da Bahia. In: Inda, H.A.V., Duarte, F.B. (Eds.), Geologia e recursos minerais do Estado da Bahia: textos básicos, ed. SME-BA/CPM, Salvador 3, 1–101.
Cameron, E.N., 1978. The lower zone of the Eastern Bushveld Complex in the Olifants River trough. J. Petrol. 19, 437–462.
Cameron, E.N., 1977. Chromite in the central sector of the Eastern Bushveld Complex, South Africa. Am. Mineral. 62, 1082–1096.
Cameron, E.N., 1980. Evolution of the lower critical zone, central sector, eastern Bushveld Complex. Econ. Geol. 75, 845–871.
Campbell, I.H., Murck, B.W., 1993. Petrology of the G and H chromitite zones in the Mountain View Area of the Stillwater Complex, Montana. J. Petrol. 34, 291–316.
Chakraborty, K.L., Chakraborty, T.L., 1984. Geological features and origin of the chromite deposits of Sukinda valley, Orissa, India. Mineral. Depos. 19, 256–265.
Chistyakova, S., Latypov, R., Zaccarini, F., 2015. Chromitite dykes in the monchegorsk layered intrusion, Russia. In situ crystallization from chromite-saturated magma flowing in conduits. J. Petrol. 56, 2395–2424.
Conceição, H., Sabaté, P., Bonin, B., 1991. The Itiúba alkaline syenite massif, Bahia State (Brazil): mineralogical, geochemical and petrological constraints – relation to the genesis of rapakivi magmatism. Precambr. Res. 51, 283–314.
Cordani, U.G., Sato, K., Nutman, A., 1999. Single zircon SHRIMP determination from Archean tonalitic rocks near Uauá, Brazil, in: S. Am. Symp. Isotopic Geology 2. Actas, Córdoba, Argentina, 27–30.
De Waal, S.A., 1975. The mineralogy, chemistry and certain aspects of reactivity of chromitite from the Bushveld igneous complex. N. Inst. Metall 1709, Randburg, South Africa, 3, 1–80.
Deus, P.B., Viana, J.S., 1982. Distrito cromitífero do Vale do Rio Jacurici. 32nd Congr. Bras. Geol., Salvador, Roteiro de Excursões 3, 44-52.
Eales, H.V., 2000. Implications of the chromium budget of the Western Limb of the Bushveld Complex. S. Afr. J. Geol. 103, 141–150.
Eales, H.V., Reynolds, I.M., 1986. Cryptic variations within chromitites of the Upper Critical zone, northwestern Bushveld Complex. Econ. Geol. 81, 1056–1066.
Ferreira Filho, C.F., Araujo, S.M., 2009. Review of Brazilian chromite deposits associated with layered intrusions: geological and petrological constraints for the origin of stratiform chromitites. Appl. Earth Sci. (Trans. Inst. Min. Metall. B) 118, 86–100.
Forien, M., Tremblay, J., Barnes, S.J., Burgisser, A., Pagé, P., 2015. The role of viscous particle segregation in forming chromite layers from slumped crystal slurries: insights from analogue experiments. J. Petrol. 56, 2425–2444.
Harley, S.L., Kelly, N.M., 2007. Zircon, tiny but timely. Elements 3, 3–18.
Irvine, T.N., 1965. Chromian spinel as petrogenetic indicator. Part 1. Theory. Can. J. Earth Sci. 2, 648–672.
Irvine, T.N., 1967. Chromium spinel as a petrogenetic indicator. Part 2: Petrologic implication. Can. J. Earth Sci. 4, 71–103.
Irvine, T.N., 1975. Crystallization sequences in the Muskox intrusion and other layered intrusions. II. Origin of chromitite layers and similar deposits of the other magmatic ores. Geochim. Cosmochim. Acta 9, 991–1020.
Irvine, T.N., 1977. Origin of chromitite layers in the Muskox intrusion and other layered intrusions: a new interpretation. Geology 5, 273–277.
Jackson, E.D., 1961. Primary Textures and Mineral Associations in the Ultramafic Zone of the Stillwater Complex, Montana. USGS Prof. Paper 358, 1-106.
Kinnaird, J.A., Kruger, F.J., Nex, P.A.M., Cawthorn, R.G., 2002. Chromitite formation – a key to understanding processes of platinum enrichment. Trans. Inst. Min. Metall. 111, 23–35.
Kosin, M., Angelim, L.A.A., Souza, J.D., Guimarães, J.T., Teixeira, L.R., Martins, A.A.M., Bento, R.V., Santos, R.A., Vasconcelos, A.M., Neves, J.P., Wanderley, A.A., Carvalho, L.M., Pereira, L.H.M., Gomes, I.P., 2004. Folha Aracaju SC.24. In: Schobbenhaus, C., Gonçalves, J.H., Santos, J.O.S., Abram, M.B., Leão Neto, R., Matos, G.M.M., Vidotti, R.M., Ramos, M.A.B., Jesus, J.D.A. de. (Eds.), Carta Geológica do Brasil ao Milionésimo, Sistema de Informações Geográficas Programa Geologia do Brasil, CPRM, Brasília, CD-ROM.
Kosin, M., Melo, R.C., Souza, J.D., Oliveira, E.P., Carvalho, M.J., Leite, C.M.M., 2003. Geologia do segmento norte do Orógeno Itabuna-Salvador-Curaçá e Guia de Excursão. Rev. Bras. Geocienc. 33, 15–26.

Li, C., Ripley, E.M., Sarkar, A., Shin, D., Maier, W.D., 2005. Origin of phlogopite-orthopyroxene inclusions in chromites from the Merensky Reef of the Bushveld Complex, South Africa. Contrib. Mineral. Petrol. 150, 119–130.
Lipin, B.R., 1993. Pressure increases, the formation of chromite seams, and the development of the ultramafic series in the Stillwater Complex, Montana. J. Petrol. 34, 955–976.
Lorand, J.P., Ceuleneer, G., 1989. Silicate and base-metal sulfide inclusions in chromites from the Maqsad area (Oman ophiolite, Gulf of Oman): a model for entrapment. Lithos 22, 173–190.
Lord, R.A., Prichard, H.M., Sá, J.H.S., Neary, C.R., 2004. Chromite geochemistry and PGE Fractionation in the Campo Formoso Complex and Ipueira-Medrado Sill, Bahia State, Brazil. Econ. Geol. 99, 339–363.
Maier, W.D., Barnes, S.J., 2008. Platinum-group elements in the UG1 and UG2 chromitites and the Bastard reef at Impala platinum mine, western Bushveld Complex. S. Afr. J. Geol. 111, 159–176.
Maier, W.D., Barnes, S.J., Groves, D.I., 2013. The Bushveld Complex, South Africa: formation of platinum–palladium, chrome and vanadium-rich layers via hydrodynamic sorting of a mobilized cumulate slurry in a large, relatively slowly cooling, subsiding magma chamber. Mineral. Depos. 48, 1–56.
Marinho, M.M., Rocha, G.F., Deus, P.B., Viana, J.S., 1986. Geologia e potencial cromitífero do Vale do Jacurici-Bahia. 34th Congr. Bras. Geol., Goiânia, Anais 5, 2074–2088.
Marques, J.C., 2001. Petrologia e Metalogênese do depósito de cromita do sill Ipueira-Medrado, Vale do Rio Jacurici-Bahia: Unpublished Ph.D. thesis, Brasília, Brazil, Universidade de Brasília, PP. 155.
Marques, J.C., Ferreira Filho, C.F., 2003. The chromite deposit of the Ipueira-Medrado Sill, São Francisco Craton, Bahia. Econ. Geol. 98, 87–108.
Marques, J.C., Ferreira-Filho, C.F., Carlson, R.W., Pimentel, M.M., 2003. Re-Os and Sm-Nd isotope and trace element constraints on the origin of the chromite deposit of the Ipueira-Medrado Sill, Bahia, Brazil. J. Petrol. 44, 659–678.
Martin, H., Peucat, J.J., Sabaté, P., Cunha, J.C., 1997. Crustal evolution in the early Archaean of South America: example of the Sete Voltas Massif, Bahia State, Brazil. Precambr. Res. 82, 35–62.
Maurel, C., Maurel, P., 1982. Etude expérimentale de la solubilité du chrome dans les bains silicates basiques et sa distribution entre liquid et minraux coexistants: conditions d'existence du spinelle chromifére. Bull. Minéral. 105, 197–202.
McDonald, J.A., 1965. Liquid immiscibility as one factor in chromite seam formation in the Bushveld Igneous Complex. Econ. Geol. 60, 1674–1685.
Melcher, F., Grum, W., Simon, G., Thalhammer, T.V., Stumpfl, E.F., 1997. Petrogenesis of the ophiolitic giant chromite deposits of Kempirsai, Kazakhstan: a study of solid and fluid inclusions in chromite. J. Petrol. 38, 1419–1458.
Mello, C.H.M.P., Durão, G., Viana, J.S., Carvalho, C.J.C., 1986. Depósitos de cromita das Fazendas Medrado e Ipueira, Município de Senhor do BonFim, Bahia. In: Schobbenhaus C., Coelho, C.E.S. (Coords.), Principais Depósitos Minerais do Brasil. DNPM/CVRD 2, 215–234.
Moller, A., O'Brien, P.J., Kennedy, A., Kroner, A., 2003. Linking growth episodes of zircon and metamorphic textures to zircon chemistry: an example from the ultrahigh-temperature granulites of Rogaland (SW Norway). In: Vance, D., Muller, W., Villa, I.M. (Eds.), Geochronology: Linking the Isotopic Record with Petrology and Textures. Geol. Soc., London, Special Publications 220, 65–81.
Mondal, S.K., 2009. Chromite and PGE deposits of Mesoarchean ultramafic–mafic suites within the greenstone belts of the Singhbhum Craton (India): implication for mantle heterogeneity and tectonic setting. J. Geol. Soc. India 73, 1–16.
Mondal, S.K., Frei, R., Ripley, E.M., 2007. Os isotope systematics of Mesoarchean chromitite-PGE deposits in the Singhbhum Craton (India): implications for the evolution of lithospheric mantle. Chem. Geol. 244, 391–408.
Mondal, S.K., Glascock, M.D., Ripley, E.M., 2002. Characteristics of Cr-spinel and whole rock geochemistry of the Nuasahi Igneous Complex, Orissa, India. In: Proc. 9th Internat. Pt-Symp., Billings, Montana, 317–320.
Mondal, S.K., Mathez, E., 2007. Origin of the UG2 chromitite layer, Bushveld Complex. J. Petrol. 48, 495–510.
Mondal, S.K., Ripley, E.M., Li, C., Frei, R., 2006. The genesis of Archean chromitites from the Nuasahi and Sukinda Massifs in the Singhbhumm Craton, India. Precambr. Res. 148, 45–66.
Naldrett, A.J., Kinnaird, J.A., Wilson, A.H., Yudovskaya, M., McQuade, S., Chunnett, G., Stanley, C., 2009. Chromite composition and PGE content of Bushveld chromitites: Part 1-the Lower and Middle Groups. Appl. Earth Sci. (Trans. Inst. Min. Metall. B) 118, 131–161.
Naldrett, A.J., Wilson, A., Kinnaird, J., Yudovskaya, M., Chunnett, G., 2012. The origin of chromitites and related PGE mineralization in the Bushveld Complex: new mineralogical and petrological constraints. Miner. Depos. 47, 209–232.
Oliveira, E.P., Escayola, M., Souza, Z.S., Bueno, J.F., Araujo, M.G.S., McNaughton, N., 2007. The Santa Luz chromite-peridotite and associated mafic dykes, Bahia-Brazil: remnants of a transitional type ophiolite related to the Paleoproterozoic (2.1 Ga) Rio Itapicuru greenstone belt? Rev. Bras. Geocienc. 37, 28–39.
Oliveira, E.P., Lafon J.M., Souza, Z.S., 1999. Archaean-Proterozoic transition in the Uauá Block, NE São Francisco Craton, Brazil: U-Pb, Pb-Pb and Nd isotope constraints. In: Int. Symp. Tecton. Braz. Geol. Soc., Lençóis, 38-40.
Oliveira, E.P., Mello, E., McNaughton, N.J., Choudhuri, A., 2002. Shrimp U-Pb age of the basement to the Rio Itapicuru Greenstone, NE São Francisco Craton. In: Congr. Bras. Geol., João Pessoa, 522.
Oliveira, E.P., Windley, B.F., McNaughton, N.J., Pimentel, M.M., Fletcher, I.R., 2004. Contrasting copper and chromium metallogenic evolution of terranes in the Paleoproterozoic Itabuna-Salvador-Curaçá orogen, São Francisco craton, Brazil: new zircon (SHRIMP) and Sm-Nd (model) ages and their significances for orogen-parallel escape tectonics. Precambr. Res. 128, 143–165.
Roach, T.A., Roeder, P.L., Hulbert, L.J., 1998. Composition of chromite in the upper chromitite, Muskox layered intrusion, northwest territories. Can. Mineral. 36, 117–135.
Rollinson, H., 1997. The Archean komatiite-related Inyala chromitite, southern Zimbabwe. Econ. Geol. 92, 98–107.
Sabaté, P., Peucat, J.J., Melo, R.C., Pereira, L.H., 1994. Datação Pb evaporação de monozircão em ortognaisse do Complexo Caraíba: expressão do acrescimento crustal transamazônico do Cinturão Salvador-Curaçá (Cráton do São Francisco, Bahia, Brasil). In: 38th Congr. Bras. Geol. Camboriú, 219.
Sack, R.O., Ghiorso, M.S., 1991. Chromite as petrogenetic indicator. In: Reviews in Mineralogy, Mineral. Soc. Am. 25, 323–352.
Santos, R.A., Souza, J.D., 1983. Projeto Mapas Metalogenéticos e de Previsão de Recursos Minerais: Serrinha, folha SC.24-Y-D (2v.) DNPM, Salvador.
Santos-Pinto, M.A.S., Peucat, J.J., Martin, H., Sabaté, P., 1998. Recycling of the Archaean continental crust: the case study of the Gavião Block, Bahia, Brazil. J. S. Am. Earth Sci. 11, 487–498.
Sharpe, M.R., Irvine, T.N., 1983. Melting relations of two Bushveld chilled margin rocks and implications for the origins of chromitite. Carnegie Inst. Wash. Yearb. 83, 295–300.
Silva, L.C., Armstrong, R., Delgado, I.M., Pimentel, M.M., Arcanjo, J.B., Melo, R.C., Teixeira, L.R., Jost, H., Pereira, L.H.M., Cardoso Filho, J.M., 2002. Reavaliação da evolução geológica em terrenos pré-cambrianos brasileiros com base em novos dados U-Pb SHRIMP. Parte I: Limite centro-oriental do Cráton São Francisco na Bahia. Rev. Bras. Geocienc. 32, 513–528.
Silva, L.C., McNaughton, N.J., Melo, R.C., Fletcher, I.R., 1997. U-Pb SHRIMP ages in the Itabuna-Caraíba TTG high-grade Complex: the first window beyond the Paleoproterozoic overprinting of the eastern Jequié craton, NE Brazil. In: Int. Symp. on Granites and Assoc. Mineral., Salvador, 282-283.
Silveira, C.J.S., Frantz, J.C., Marques, J.C., Queiroz, W.J.A., Roos, S., Peixoto, V.M., 2015. Geocronologia U-Pb em zircão de rochas intrusivas e de embasamento na região do Vale do Jacurici, Cráton do São Francisco, Bahia. J. Braz. Geol. 45, 453–474.
Spandler, C., Mavrogenes, J., Arculus, R., 2005. Origin of chromitites in layered intrusions: evidence from chromite-hosted melt inclusions from the Stillwater Complex. Geology 33, 893–896.
Stowe, C.W., 1994. Compositions and tectonic settings of chromite deposits through time. Econ. Geol. 89, 528–546.
Teixeira, W., Sabaté, P., Barbosa, J., Noce, C.M., Carneiro, M.A., 2000. Archean and Paleoproterozoic tectonic evolution of the São Francisco Craton, Brazil. In: Cordani, U.G., Milani, E.J., Thomaz Filho, A., Campos, D.A. (Eds.), Tectonic Evolution of South America, Int. Geol. Congr., Rio de Janeiro, 101–137.
Ulmer, G.C., 1969. Experimental investigations of chromite spinels. In: Wilson, H.D. B., (Eds.), Magmatic ore deposits. Econ. Geol. Monograph, Lancaster, 114-131.
Voordouw, R., Gutzmer, J., Beukes, N.J., 2009. Intrusive origin for Upper Group (UG1, UG2) stratiform chromitite seams in the Dwars River area, Bushveld Complex, South Africa. Mineral. Petrol. 97, 75–94.
Wilson, A.H., 1982. The geology of the Great 'Dyke' Zimbabwe: the ultramafic rocks. J. Petrol. 23, 240–292.
Yudovskaya, M.A., Naldrett, A.J., Woolfe, J.A.S., Costin, G., Kinnaird, J.A., 2015. Reverse Compositional Zoning in the Uitkomst Chromitites as an Indication of Crystallization in a Magmatic Conduit. J. Petrol. 56, 2373–2394.